UNIVERSITÀ DI PARMA

UNIVERSITÀ DI PARMA

DOTTORATO DI RICERCA IN BIOTECNOLOGIE E BIOSCIENZE

CICLO XXXIV

Expression profiling of the developing rabbit lung

Coordinatore:

Chiar.mo Prof. Marco Ventura

Tutor:

Chiar.ma Prof. Barbara Montanini

Dr. Gino Villetti

Dottorando: Francesca Ricci

Anno accademico 2018/2021

Abstract

Bronchopulmonary dysplasia (BPD) is the most common respiratory morbidity in preterm neonates with an incidence of 5–68%, which increases significantly with declining gestational age (GA). Despite advances in neonatal care having resulted in improved survival rates of premature infants, limited progress has been made in reducing BPD rates. The clinical BPD phenotype is the result of a complex multifactorial process in which various pre- and postnatal factors compromise normal development of the immature lung. Understanding how the alveoli and capillary network develop and how these mechanisms are disrupted in BPD is critical for developing efficient therapies. In this scenario, animal models are essential tools for the preclinical development of pharmacological treatments. In the last years, in Chiesi laboratories, a hyperoxia-exposed preterm rabbit model of BPD has been validated. This model represents a suitable lab preclinical tool for mimicking the clinical BPD phenotype to test new pharmacological treatments. However, the molecular characterization of rabbit lung development is lacking. The main aim of this study was to demonstrate the translational power of the preterm rabbit as BPD model by a multi-disciplinary approach to i) characterize histological and molecular changes during the physiological rabbit lung development ii) evaluate the prematurity impact on rabbit lung development, and iii) compare rabbit and mouse lung developmental expression. During the PhD project, we have finalized RNA sequencing analysis of lung samples collected at different time points of GA that correspond to different lung developmental stages of rabbit (canalicular, saccular and alveolar phases). We identified genes and pathways related to processes involved in lung development. Weighted correlation network analysis (WCNA) showed a progressive transcriptomic development profile, starting from pseudo glandular up to the alveolar phase. These results were confirmed by histological analysis and showed a significant similarity of our data with the main gene/protein-set involved in the normal lung development of humans. Prematurity impact on rabbit lung physiological gene expression was evaluated comparing the transcriptomic profiles of preterm and age-matched term pups. Pathway enrichment analysis of

differentially expressed genes (DEG) lists highlighted that genes up-regulated in the preterm animals in comparison to the age-matched term pups were mainly enriched in terms of immune system related-pathways. In addition, immune system activation and developmental patterns are delayed as a result of premature delivery in comparison to the term birth. In order to demonstrate the translational power of the preterm rabbit as a BPD model, we compared rabbit data with currently literature-available records from a preclinical transcriptomic study on lung development in mice, the most used animals for preclinical study on BPD. The results showed that the expression profile at preterm and term birth in both species was similar. Common enriched pathways are present in mice and rabbits born in both preterm and term conditions, despite their different lung developmental phases. No enriched common pathways emerged from the comparison between preterm rabbits and term mice. Rodents born at term in the saccular phase have structurally immature lungs, but they are functionally mature and fully capable of extrauterine survival, contrary to preterm rabbits that have structurally and functionally immature lungs as preterm neonates. This result supports the high translational power of the preterm rabbit as a suitable animal model for studying the dysregulation of lung development-related pathways, leading to BPD.

Table of Contents

1 Introduction

1.1 Phases of human lung development

Human gestation has a physiological duration of 40 weeks (9 months), and the fetal growth is divided into three different phases: i) zygote development, from fertilization to the end of the 2nd week, ii) embryo period that goes from 3rd to 8th weeks followed by iii) the fetal period that lasts until birth (40th week)[1] (Figure 1).

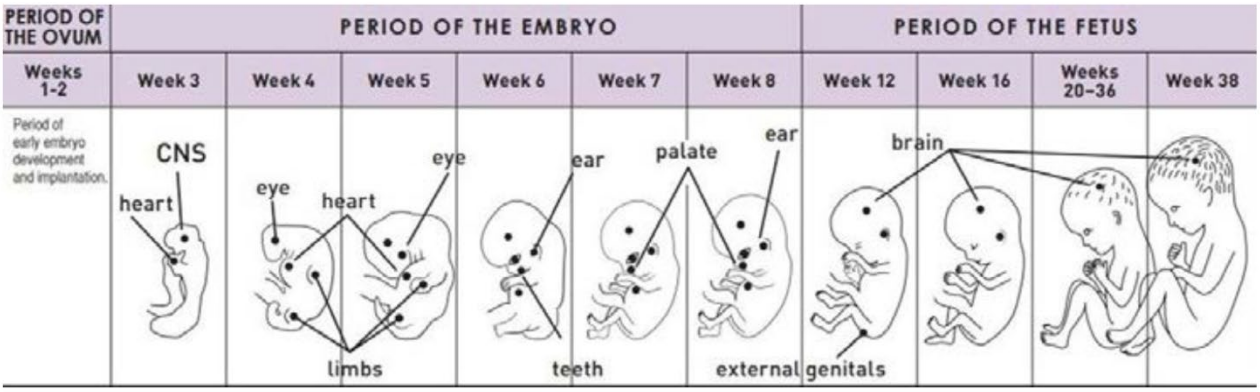

Figure 1. Gestation phases (Adapted from Keith L. Moore et al. 2013)

The development of the respiratory system begins at about week 4 of gestation and continues up to two years of life[2]. The mature lung is a complex structure composed of endodermal and mesodermal cells that undergo an intricated developmental process determined by functional integration of genetic, physical and chemical changes. All components during development follow a predictable timeline during fetal development. After the early embryonic stage, characterized by a branching morphogenesis process, four phases of lung development occur in prenatal lung development: pseudoglandular, canalicular, saccular, and alveolar periods[3,4]. (Figure 2)

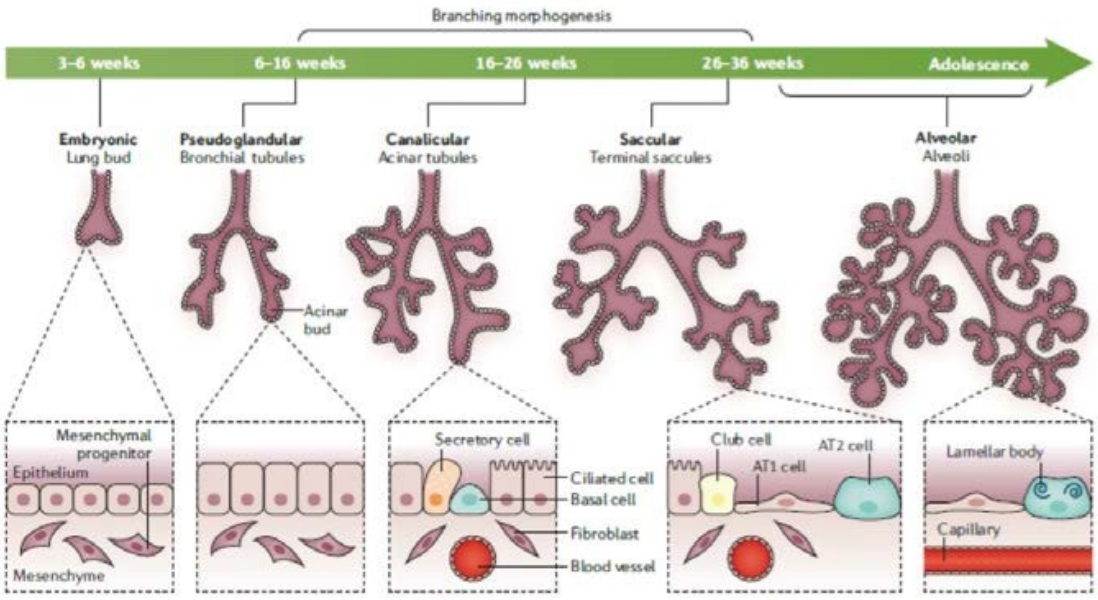

Figure 2. Phases of human lung development (Adapted from Thebeau Jobe et al. 2021)

- Embryonic period (from 4th to 6th week)

The mesenchyme invasion of lung buds, which emerge as ventral outgrowths of the primitive foregut, begins in the embryonic period. The epithelial cells of the foregut endoderm give rise to the trachea. The trachea then divides into the right and left main bronchi and then into lobar and segmental bronchi[5].In this period, vasculogenesis starts around the buds of the airways[6].

- Pseudoglandular period (from 6th to 16th week)

During this stage, airway and vascular networks undergo further branching and adult structures take shape thanks to a progressive differentiation of epithelial cells[6].This stage ends with a completed branched structure, base for the future bronchial tree and the pre-acinar structures, including pre-acinar airway, pulmonary arteries, and veins [6,7].

- Canalicular period (from 16th to 24th week)

This period is characterized by pulmonary parenchyma development and respiratory tree extension in diameter and length, along with vascularization and angiogenesis of the airway [7]. Additionally, in this stage, respiratory bronchioles, alveolar ducts and primitive alveoli are formed[8] . At the 20th week of gestation, the epithelial cells differentiate in type 1 and 2 pneumocytes. Alveolar type I (ATI) cells are large flat cells that cover the majority of the alveolar surface (95%), ensuring an efficient gas exchange[9] .Alveolar type II (AT2) cells support the correct lung development and produce, store and secrete the pulmonary surfactant[10] , whose primary function is to increase the compliance of the lungs by reducing alveolar surface tension[11].

- Saccular period (from 24th to 36th week)

During this stage, the widening of peripheral airways and the consequent dilatation of acinar tubules lead to the formation of 'saccule' structures and thinner airway walls[8].These saccules generate the alveolar ducts and the peripheral alveolar sacs[2].In the meantime, AT2 cells increase their surfactant synthesis and secretion[2],a key step in determining whether the newborn lung can sustain gas exchange without collapsing[12].

- Alveolar period (from 36th week until 2 years of life)

After the development of primary alveoli through the formation of secondary crests generates a further expansion of the gas-exchange surface. Primitive saccules develop low ridges (primary septa) that subdivide the saccule in alveolar ducts containing primary alveoli and outpouchings between the ridges (secondary septa/crests) that establish secondary alveoli[13].Alveolar multiplication continues up to 2–3 years of age, while alveolar surface increase until adolescence[8] .

1.2 Molecular regulation of lung development

The timing of lung maturation is controlled precisely by complex genetic and pathway programs[14] (Figure. 3). The interaction between the airway epithelium and surrounding mesenchyme regulates the lung developmental process coordinated by transcriptional and growth factors, and extracellular matrix[15].Due to ethical limitations to performing studies on human fetuses, most of the knowledge on cellular and molecular mechanisms of lung development has been improved through genetics and genomics studies on animals.

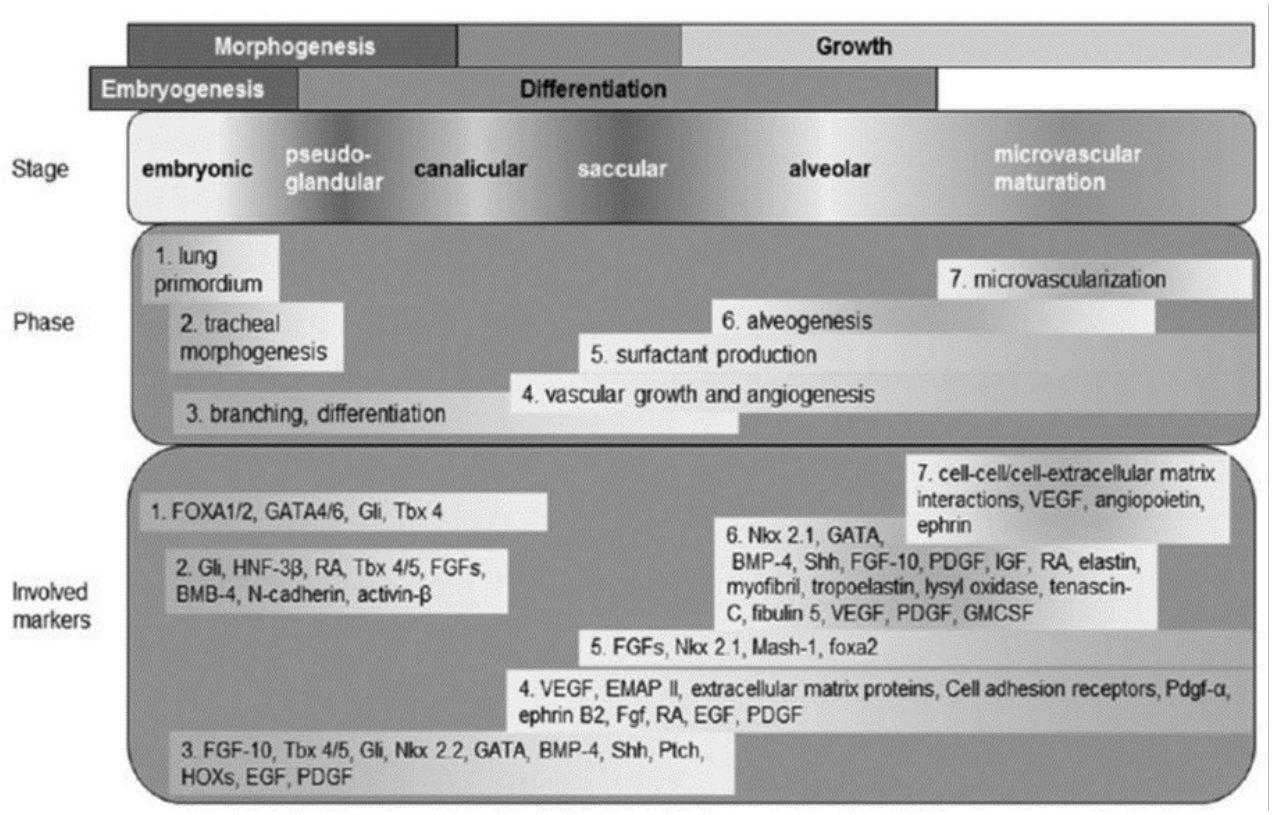

Figure 3. Molecular markers in respiratory development

Lung developmental process is mediated by changes in gene expression, which is controlled by several transcription factors. Multiple transcription factor families are involved in the process, including Forkhead box (FOX), Nkx and GATA families. Important transcription factors as

hepatocyte nuclear factor 3ß (HNF-3ß or foxa2) and thyroid transcription factor-1 (TTF-1 or Nkx2.1) are involved in the early lung organogenesis[16]. Nkx2.1 acts in concert with HOX family to specify and control the transcriptome of the respiratory lineage. Fibroblast growth factor (FGF) signals promote the initial segregation of the ventral foregut in the lung[17,18] via Mitogen-activated protein kinases (MAPK) and Akt pathways[19]. In the early separation of the foregut into distinct tracheal and esophageal, bone morphogenetic protein (BMP)/Wnt and Sonic Hedgehog (Shh) pathways are essential to guarantee the process. Retinoic acid (RA), FGF, Wnt and Transforming growth factor (TGFb) pathways control the initial growth of the primary lung buds[20]. During the pseudoglandular stage the fetal lung grows by branching morphogenesis. Coordinated development of the conducting and distal airways is a vital process during which both the epithelial and mesenchymal compartments play integral roles. During this process, a complex cross-talk between epithelial and mesenchymal components is involved[20,21]. This interaction is regulated by key signaling factors: especially FGF-10 and FGF-7, transforming TGF-ß, Shh, vascular endothelial growth factor (VEGF), epidermal growth factor (EGF), platelet-derived growth factor (PDGF) and BMP-4, with their respective receptors and intracellular signaling molecules[21].

Differentiation of the respiratory epithelium begins in the fetal stage and proceeds into the postnatal period[22]. GATA transcription factors and TTF-1 play a critical role in promoting epithelial progenitors cell differentiation in the ciliated, goblet and basal cells starting from sex determining-region Y-box 2 (SOX2) proximal airway cells[15,22–24]. Whereas the distal epithelium progenitors SOX9/ID2 in lung tips undergo septation and expansion into alveoli differentiating in gas-exchanging squamous ATI cells and surfactant producing cuboidal ATII cells[22,24]. During the saccular stage, alveolar sacs made by dichotomous branching tubules go through an alveolar septation mechanism in order to extend the exchange surface. At this stage, α-smooth muscle actin $(\alpha SMA)^{+}$ myofibroblasts appear in the immature secondary septa, and the expression of extracellular matrix (ECM) components such as elastin increases[15]. The deposition of elastin and the presence of alveolar

myofibroblasts are markers of secondary septation. The main factor that controls this process of alveolarization is PDGF-A and its receptor PDGFR-alfa[21,25]. In parallel to lung development, a three-dimensional structure of capillary network grows to enable the exchange of respiratory gases. Cell-cell interactions, angiopoietin and ephrin transcription, and growth factors as VEGF are involved in pulmonary vascularization[26].

1.3 Prematurity and its effects on lung development and neonatal chronic diseases

Premature birth significantly impacts normal lung development. A premature infant is born before 37th weeks of gestation (full term is 37 to 42 weeks). Infants born before 32 weeks gestation are defined as ‘‘very preterm’’, while infants born before 28 weeks gestation are considered ‘‘extremely preterm”[27,28].Preterm babies are born in late canalicular or saccular stage of lung development when the alveolarization and the proliferation of the capillary network is still incomplete. Prematurity and post-natal factors could lead to the two main respiratory pathologies of premature infants: neonatal respiratory distress syndrome (nRDS) and bronchopulmonary dysplasia (BPD). Nowadays, in the neonatal intensive care unit (NICU) the preterm delivery management involves the administration of antenatal corticosteroids, artificial breathing support, and exogenous surfactant replacement therapy (SRT)[29,30]. Although the progress in medical care had an impact on improved survival for the smallest infants with nRDS, an increase in rates of bronchopulmonary dysplasia (BPD) has been reported[31,32]..

Lung structural and functional immaturity at birth is crucial for developing lung disease in preterm neonates with an important long term impact on the respiratory system. Recent longitudinal studies on childhood showed that survivors of very preterm birth develop chronic obstructive pulmonary disease (COPD)[33]. The extrauterine transition requires immediate and extensive adaptations to guarantee physiological autonomy for the newborn. Prior to birth, innate immune responses and

surfactant production are critical and connected processes that positively influence lung maturation necessary for respiration and survival after birth[34]. In addition, the antioxidant defense enzymes, which mature in parallel with the surfactant system, show an important role to prepare a fetus for its pulmonary adaptation at term birth[35].The lack of this preparation in the preterm neonate requires endogenous adaptive strategies. Nguyen et al. demonstrated that systemic immunity follows a distinct developmental trajectory after preterm birth, underling that immature immune system in preterm neonates adapts after birth, and various factors influence it in the postnatal period (external environment, variable antibiotic treatment, and impaired organ function)[36].ROS susceptibility has been observed in preterm babies[37] and hypoxia/reoxygenation episodes in early life could sustain a proinflammatory cascade[38] In addition, several studies demonstrated that preterm babies have high intermittent hypoxic episodes due to immature respiratory control[35]. The postnatal and early life adaptations in preterm neonate impact the normal lung growth and development, which might promote a shift from the "normal" lung function trajectory. Currently, several studies are focused on the monitoring of the long-term medical follow-up of people born preterm[33].

1.4 Bronchopulmonary Dysplasia

Currently, most of the extremely preterm neonates survive, but they often develop BPD, a chronic lung dysfunction characterized by an arrest on the development of the alveoli, airways, and pulmonary vasculature. BPD was recognized for the first time in the 1960s by Dr. Northway[40.] At that time, the management of these babies, such as aggressive ventilation and high oxygen levels for at least 7 days, implicated the developing of a fibrotic disease, now defined as "Old BPD"[40].

Over the past 50 years, the advances in medical care such as the use of antenatal corticosteroids, non-invasive respiratory support devices and surfactant treatments, have allowed increasing the surival of preterm infants. In parallel with the advances in medical care approaches, the characteristics of BPD

have evolved since the initial descriptions of the disease[41,42] .Today, the “Old BPD” has been replaced by “New BPD”. “New BPD” is described as a developmental arrest alveolar hypoplasia, decreased septation, dysregulated development of pulmonary vasculature, and abnormalities in respiratory function[43,44].Currently, even if the rate of survival is increasing even for extremely preterm babies, the incidence of BPD is about 40%, remaining the most common adverse outcome of prematurity[40,41,44,45].Neonatologists have to rely for their diagnosis on indirect clinical features, such as oxygen requirement and ventilator support, because they cannot access histological data that allow evaluating the pathology[46]. Indeed, the worldwide accepted definition of BPD is based on the “requirement for mechanical ventilation and oxygen dependence at 28 days or 36 weeks of postmenstrual age of life (PMA)”[44,47] .Thus, the definition is not based on BPD pathology but on its therapy. The National Institutes of Health and the Office of Rare Diseases have improved the classification of BPD, including a severity scale. Therefore, it is now subdivided into mild, moderate, and severe according to the respiratory support provided at 36 weeks PMA among very preterm infants treated with supplemental oxygen for at least 28 days[42].

Several prenatal and postnatal factors are involved in the development of BPD[48–50] (Figure 5),but prematurity remains the main risk factor and the incidence of BPD increases as gestational age decreases. BPD is a multifactorial disease recognized as the result of an aberrant reparative response to both antenatal injury and repetitive postnatal injury to the developing lungs[51].However, the BPD pathophysiology has not been fully understood yet, and no therapies have been approved for prevention or treatment. For these reasons, suitable animal models are needed to investigate the pathobiology of BPD which will provide novel therapeutic targets.

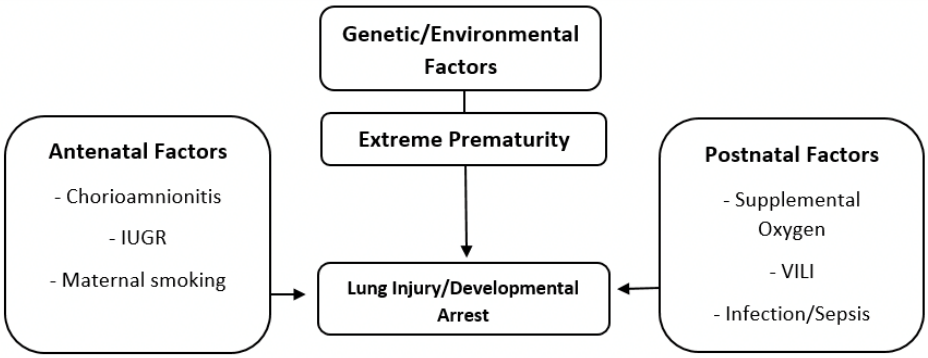

Figure. 5. *Prenatal and postnatal risk factors in developing BPD (Image adapted from Alan Jobe.) Intra Uterin Growth Restriction (IUGR); Ventilator – Induced Lung Injury (VILI).*

1.4.1 Translation of BPD phenotype in animal models

Several animal species have been exploited for developing preclinical models of neonatal diseases[52–54] .It is essential to have animal models that mimic some of the main features that contribute to the BPD development to characterize the BPD pathophysiology: growth restriction, hyperoxia, prematurity, perinatal inflammation. In the last decades, large and small animals have been used to mimic the BPD phenotype[55,56] .(Figure 6).

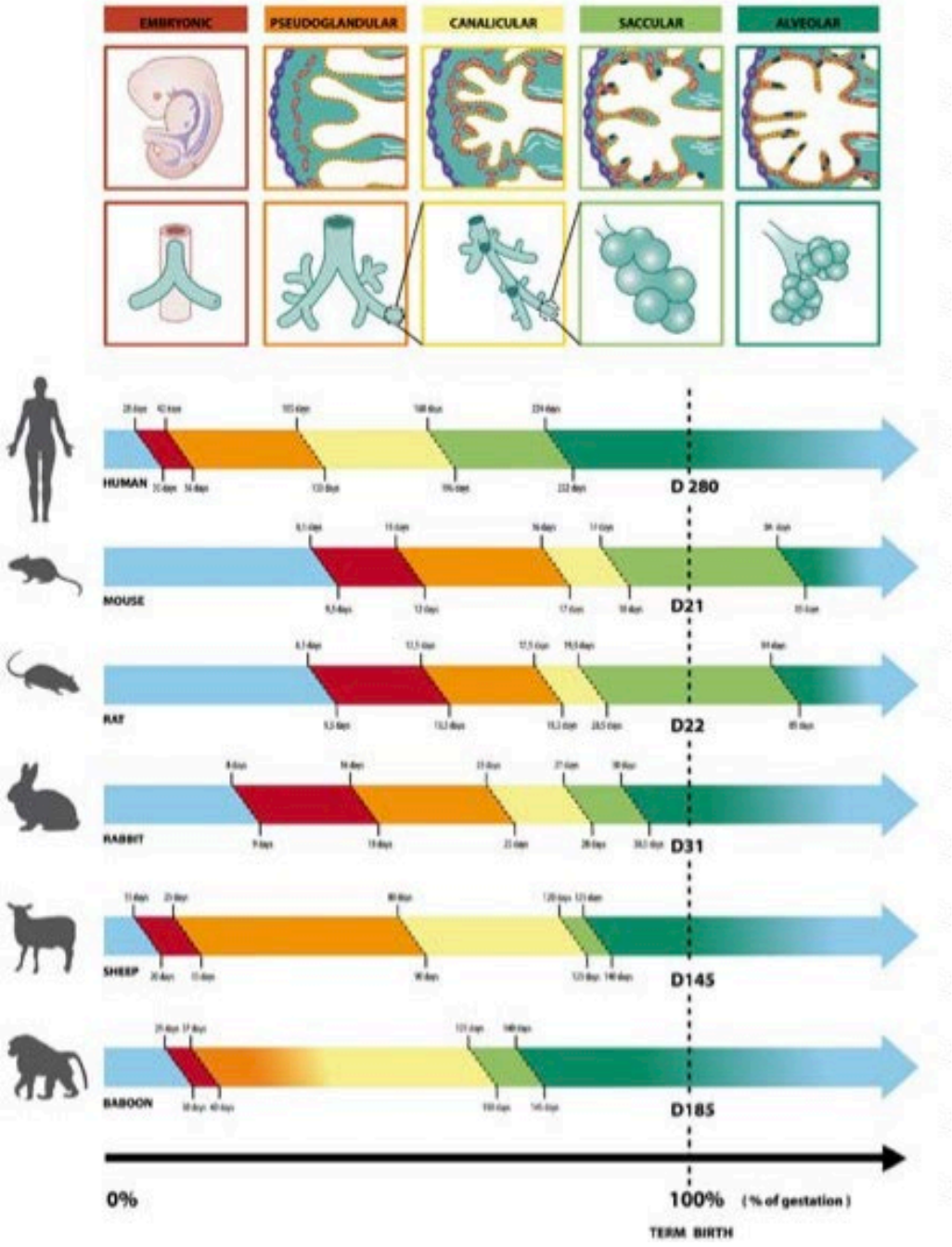

Figure 6. Mammalian lung development (adapted from Salaets et al)

All models have some advantages and limitations which should be carefully considered. Small animal models, such as mice and rats, are the most used species to mimic neonatal BPD due to their limited maintenance cost and short gestational period (21 days for mice, 22 days for rats) with large litter size, making them suitable for investigating the molecular pathways involved in specific aspects of BPD[53,57] .Unlike human neonates, who are born at term in the alveolar phase, mice and rats are born

at term in the saccular stage that is equivalent to that of preterm neonate. Although rodents are born at term in the saccular stage, they have structurally immature but functionally mature lungs. Rodents pups delivered during the saccular stage are fully capable of extrauterine survival; on the contrary, human neonates delivered during the saccular stage are at high risk for developing respiratory distress syndrome and chronic lung disease due to pulmonary immaturity[52,53]. However, considering that they are born at term in the same lung developmental phase of premature babies eliminates the need for induced preterm birth to investigate an immature lung. This aspect makes them attractive models for investigating new pharmacological BPD treatment, but on the other hand, reduces their translational power significantly.

Instead, big animal models such as lambs, macaques, and baboons showed higher translational power than small animals. The physiological lung development phases of big animals mainly reflects the human ones. They are born at term in the alveolar phase, and their developmental stages timeline is comparable to humans. Moreover, they can be delivered prematurely[58,59] and managed with clinical-like supportive conditions. Despite these strengths, these species have several disadvantages related to their long gestation period (152 days for lambs, 166 days for macaques, and 180 days for baboons), a small litter size, high maintenance costs, highly intensive care requirements, and ethical limitations, especially for non-human primates[58,59].In this scenario, medium-size animals as rabbits represent a potentially good compromise between small and large animals.

1.4.2 The Preterm Rabbit Model

Rabbits are a practical compromise between small and large animal models. They are easy to house, cost-effective, with a relatively short gestation period (31 days), and large litter size. In addition, rabbits are born at term in the alveolar phase as occurs in large animals and humans. They can be delivered prematurely in contrast to mice and rats[60].However, the physiological development of the rabbit lung has not been yet characterized at the molecular level. Salaets T. et al. have recently applied

transcriptome analysis to the rabbit pup lung tissue for the first time. However, they did not report any biomolecular marker related to different stages of normal lung development, which could be relevant for setting the stage for a meaningful investigation of molecular processes triggered by prematurity (and/or external insults)[61] .

Rabbit pups can be delivered through the caesarian section on the 28th day of gestation, during the saccular phase of lung development. At this stage of development, premature rabbits have structural and functional immature lungs as human preterm babies[52,61].The size of preterm rabbits allows the use of numerous types of manipulations such as surfactant replacement therapy (SRT), hyperoxia exposure, intra-tracheal injection of drugs, gavage feeding, and short periods of mechanical ventilation[61,62] .All these aspects make the preterm rabbit model a suitable model for investigating innovative strategies for BPD treatment with high translational power. However, the preterm rabbit model shows some limitations: i) it is not commonly used as rodent models, ii) reagents and tools are not largely available, iii) long-term ventilation cannot be performed because of its small size, and iv) it is less characterized at the molecular level compared to rodent models.

In the last decades, a widely used BPD rabbit model is the hyperoxia-exposed preterm rabbit[62,63] that includes two of the main triggers of BPD phenotype: prematurity and hyperoxia[62–64] .Preterm pups are maintained under hyperoxia condition (fraction of inspired oxygen [FiO_2] > 95%) for 7 days. After prolonged hyperoxia exposure, animals show several BPD features, including decreased respiratory functional capacity and an abnormal tissue structure. Moreover, hyperoxia-exposed preterm rabbis display the first symptoms of pulmonary hypertension (PH), as demonstrated by a reduced ratio in pulmonary artery acceleration time (PAAT) and ejection time (PAET), which is indirectly correlated with pressure in the right ventricle of the heart[62–64]. However, the hyperoxia-exposed animal model presents some limitations. FiO_2 > 95% used to induce hyperoxia damage is a high oxygen concentration which is no more the standard care in NICUs. In addition, the short timeline to 7 days cannot permit to study long-term outcomes, as happen in small and large animal

models[62–64] ; thus, it is useful to test preventative drugs rather than therapeutic treatments. Moreover, delivery at the 28th day of gestation does not closely mimic the prematurity condition of extremely preterm neonates. Pups born on the 28th day can spontaneously breathe without ventilation support. The induction of preterm delivery at 27th days of gestation has been considered for better mimicking extremely preterm babies, but their management is very challenging. Finally, this model does not incorporate prenatal interventions, such as antenatal steroids administration, and post-natal ones, as caffeine administration. Taking into consideration all these advantages and disadvantages, the preterm rabbit model represents a suitable model to test new therapies for BPD prevention and treatment.

1.5 State of art on omics in lung development characterization with focus on animal model

Due to the intrinsic limitations of performing studies on human fetuses, animal models can improve knowledge on the molecular and signaling pathways that control normal lung development. In the last decades, -omics studies have improved knowledge of lung development processes across species. Several omics techniques have been applied in small and big animals: microarray, proteomic and RNAseq technologies. Microarray and proteomic technologies have been used to characterize the biomolecular aspects of lung development in murine models[65–6869–71]. Beauchemin et al., using the microarray technique, characterized the temporal gene expression of 26 pre- and post-natal time points during normal lung development in three different mice strains[69]. In addition, proteomics analysis[70] of murine lungs from embryonic to early adult ages identified several pathways involved in lung development. In particular, they reported involvement of the cell proliferation pathway in the early stage of lung development, activation of the immune system in response to a nonsterile oxygen-rich ambient environment at birth and a critical role of the surfactant metabolism. These results were

also confirmed by Yan et al. They characterized the mRNA expression in mice born E15.5 to Postnatal Day 0 (PN0). The results showed an activation of the cell adhesion, vasculature development and lipid metabolism/transport pathways during the saccular stage of normal lung development (Figure 4). In addition, in the later stage of lung development, pathways related to innate defense/immune responses were induced. In contrast, expression of RNAs associated with the cell cycle and chromatin assembly was repressed during the prenatal phase of lung maturation[67].

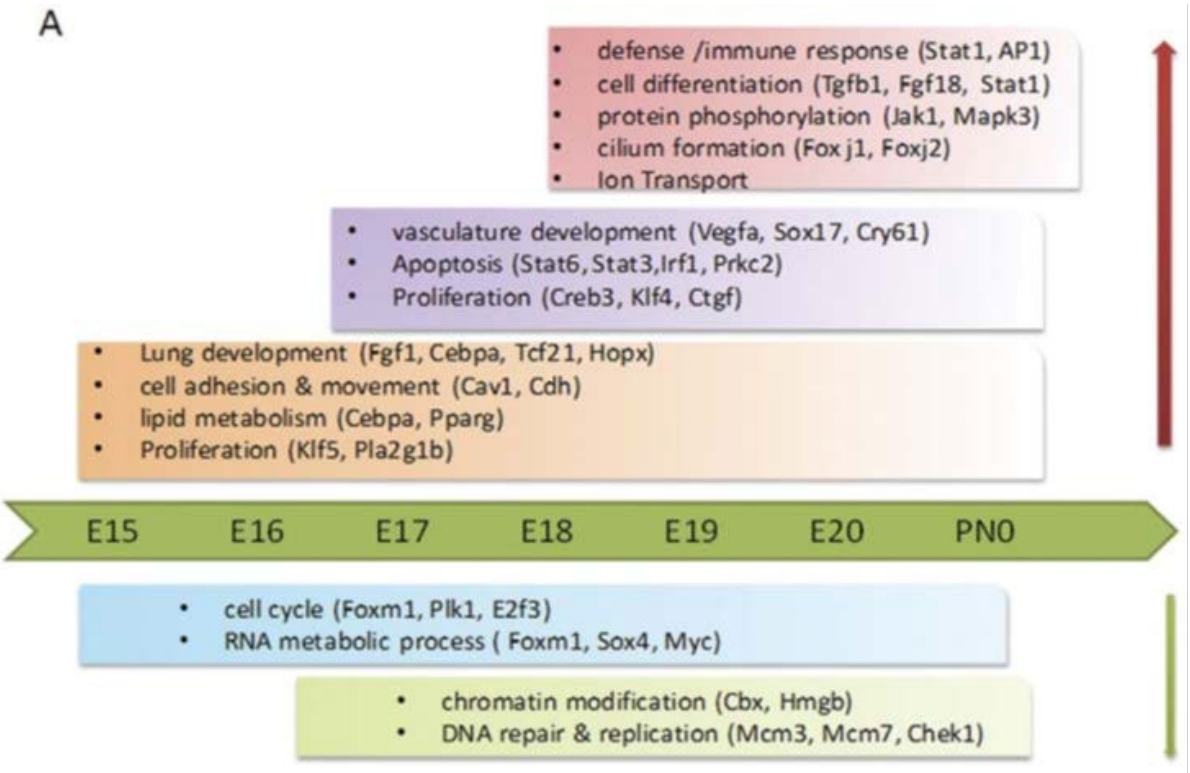

Figure 4. Molecular markers in mice lung development

Moreover, RNA sequencing analyses have been performed on lung tissue collected at different developmental stages in piglet and macaque[72,73].Long J et al. applied RNA sequencing on lung tissue of fetal (the last day of perinatal) and neonatal (two days postnatal) piglets. In the neonatal samples, they reported enrichment pathways related to cell proliferation, immune response, hypoxia response and mitochondrial activation[72]. These results were in line with the results obtained by RNA

sequencing on lung tissues of rhesus macaques from foetuses at gestation of 45 days to postnatal at 7 days reported by Yu et al.. In this study, internal growth signaling was identified as mainly associated with the early stage of lung development, such as cell cycle, while the middle and late stages were characterized by pathways related to the response at the external stress signaling[72]. Kho A.T. et al. characterized the gene expression profile during early human lung development (pseudoglandular and canalicular phases)[74] applying RNA sequencing technique. They reported as main pathways, in good agreement with preclinical studies, chemokine-immunologic processes activation and induction of surfactant gene expression. However, lung development studies performed on human lung samples are still relatively rare and focused only on the earlier phases of lung development[65].

The application of omics techniques to improve knowledge on normal lung development has an important role in understanding how the alveoli develop and how these mechanisms are disrupted in chronic lung diseases as BPD characterized by an arrest of lung development. For this reason, the development of reliable animal models and a deeper understanding of the molecular basis of the BPD pathophysiology is required to enable the investigation and development of new treatments.

2 Aim of the study

Suitable animal models could improve knowledge on the molecular and signaling pathways that control the normal lung development. Preclinical research that focuses on the identification of pathways that are involved in in-utero lung development and disrupted by respiratory disorders, congenital defects in human neonates and pre-term birth, could lead to novel therapeutic strategies for BPD. In our study, we reported a comprehensive characterization of the normal rabbit lung development and the impact of the prematurity on the molecular pathways that regulate the postnatal lung structure.

3 Materials and methods

3.1 *In-vivo* protocol

Timed pregnant rabbits (New Zealand White) were provided by Charles River Laboratories (Domaine des Oncins, France). All experiments were approved by the intramural Animal Welfare Body and the Italian Ministry of Health (Prot. n° 744/2017-PR and n° 899/2018-PR) and complied with the European regulations for animal care. Pregnancy was confirmed with ultrasounds at 12-14 days post artificial insemination at the supplier's facility. Does were maintained with food and water ad libitum until the Caesarian section (C-section) was performed, or natural birth occurred on the 31st day of gestation. When natural delivery at term (31st GA) was allowed, does were placed in special cages equipped with an external box where to build their nest.

3.2 C-section and lung tissue collection

On day 28th of gestation, does were initially sedated with intramuscular (i.m.) medetomidine 2 mg/kg (Domitor®, Orion Pharma, Finland). Ten minutes later, they received i.m. 25 mg/kg of ketamine (Imalgene 1000®, Merial, France) and 5 mg/kg of xylazine (Rompun®, Bayer, Germany). Subsequently, does were euthanized with an overdose of pentothal sodium (50 mg/kg, MSD Animal

Health, USA). After death occurred, the abdomen was immediately opened, and the uterus was exposed to extract all pups through hysterectomy. Pups lung samples were collected at different prenatal and postnatal ages. Fetal (F) pups were delivered through C-section at different days of gestation (20^{th}, 23^{rd}, 25^{th}, 27^{th}, 28^{th}, and 29^{th} day) (Figure 7). After birth, the whole lungs were immediately surgically dissected in order to avoid the contact with the surrounding environment. Instead, preterm (P) pups were delivered through C-section on the 28th day of gestation and maintained in custom-made incubators (Okolab, Italy) at 32°C, 50-60% relative humidity and 21% of oxygen up to 7 days, as described by Salaets et al. (Salaets et al., Am J Physiol Lung Cell Mol Physiol, 2019). Pups were fed twice daily via an orogastric tube (Vygon 3.5 Fr, France) with a milk replacer (Day One®, Protein 30%, Fat 50%; FoxValley, USA) and additional probiotics (25 mg/ml) (Bio-Lapis®; Probiotics International Ltd, UK), whereas immunoglobulins (Col-o-Cat®, SanoBest, Netherlands; 15 mg/ml) were added only during the first 2 days of life. The volume of feeds was increased from a total of 80 ml/kg/day on the day of birth, 100 ml/kg/day on day 1, 150 ml/kg/day on day 2, and 200 ml/kg/day from day 3 to day 7. On day 2, vitamin K was administered i.m. (0.25 mg/kg, Izokappa®; Izo s.r.l., Italy). Whole lung samples were then harvested from preterm pups at precise postnatal ages (1 h, 3, and 7 days) in the first week of life. Term (T) rabbits were naturally delivered at term on the 31^{st} day of gestation. After birth, pups were maintained with their mothers at room air in individual cages up to 11 days of postnatal age (31^{st} + 11 days). Lung samples were then collected from term pups at birth (31^{st} day) and at precise postnatal ages (35^{th}, 37^{th} and 42^{nd} day of gestation). All pups were euthanized with a pentothal sodium overdose before lung harvesting. At least three lung samples were collected at each gestational and postnatal time point from different experimental sessions. Lungs were completely removed, weighted, and selectively separated into the right and the left part. Right lungs were dedicated to transcriptomic analysis, while histological analysis was performed on the left ones. Exceptionally for very early fetal time points (20 and 23 gestational days), transcriptomic and histological analyses were performed on different whole lungs, due to their reduced size.

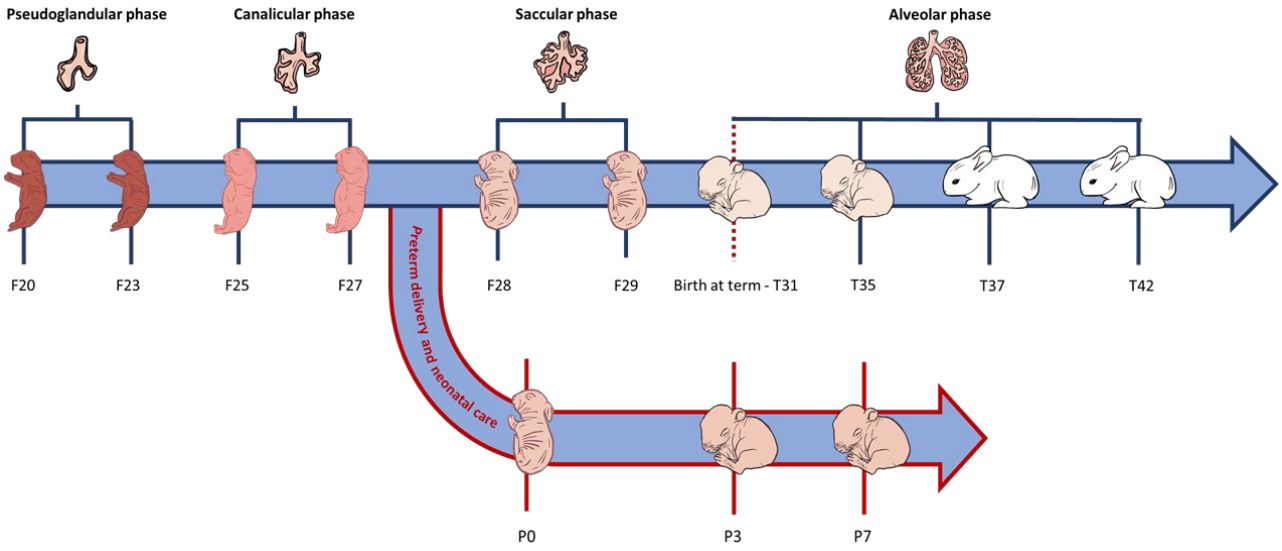

Figure 7. Scheme of the experimental timeline. Samples were collected at different lung developmental phases. Fetal (F) animals were delivered on the 20th, 23th, 25th, 27th, 28th, 29th day of gestation, through C-section, and lungs were harvested immediately after birth, before their first breath. Term (T) pups were naturally delivered at term on the 31th day of gestation and they were maintained with mothers until lung collection at birth (T31), 4 days (T35), 6 days (T37), and 11 days (T42) after delivery. Preterm (P) rabbits were delivered through C-section on the 28th day of gestation and maintained with 21% oxygen in custom-made incubators until lung collection was performed 1 hour (P0), 3 (P3) or 7 (P7) days after preterm birth.

3.3 Lung tissue morphometry

Lungs were fixed with 10% buffer formalin (Sigma-Aldrich, Germany) for at least 4 hours under constant pressure (25 cmH2O). After 48 hours of formalin fixation, lung samples were dehydrated in graded alcohol solutions, xylene clarified, and paraffin-embedded with the dorsal surface of the slice down. Serial sections 5 µm thick were obtained using a rotary microtome and stained with Hematoxylin and Eosin (H&E), Masson Thrichrome (TM), or Orcein, according to the manufacturer's specifications (Histo-Line Laboratories). Histological slides were acquired as whole slide image (WSI) by digital slide scanner (Nanozoomer S-60, Hamamatsu, Japan). The lung developmental process was histomorphometrically analysed by calculating the tissue density (TD),

the radial alveolar count (RAC), and the medial thickness of pre- and intra-acinar arteries (MT%). The tissue density was determined using an application developed within Visiopharm image analysis software (Hoersholm, Denmark). Applying a threshold-based mask on lung section, the stained tissue area of the WSI was measured foresaw the exclusion of air spaces and the inclusion of cells and nuclei. The percentage stained area was calculated dividing the stained area by the total selected area (x 100). The other two parameters were manually calculated on H&E stained sections, by the use of the Hamamatsu viewer. The RAC was performed by drawing a perpendicular line from the lumen of the terminal bronchiole to the nearest connective tissue septum or pleural margin, and the number of saccules or alveoli crossed by this line was counted (Figure 8. A, B)[75,76] .

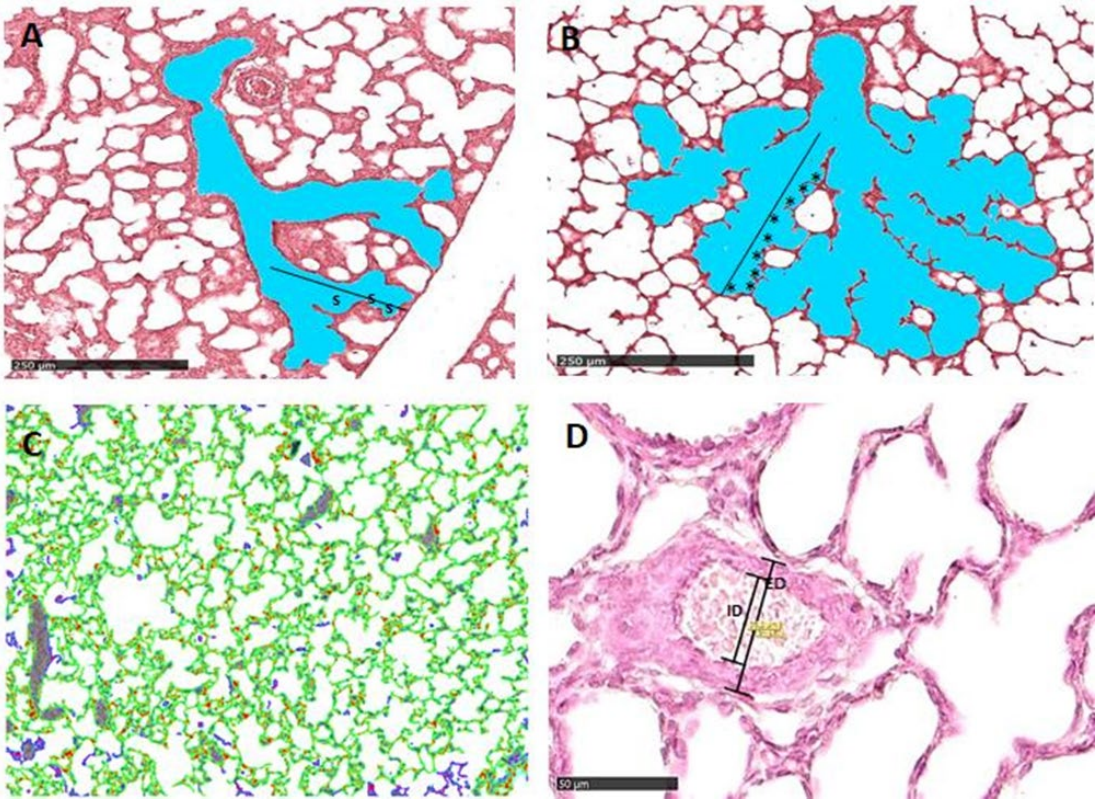

*Figure 8. Methods used for the evaluation of the histomorphometric parameters.A-B. Histological images of the respiratory portion of the lung during the saccular (A) and the alveolar phase (B) showing the method of measuring the radial alveolar count (RAC). A perpendicular line was drawn from the lumen of the terminal bronchiole to the nearest connective tissue septum and the number of saccules (s) or alveoli (*) crossed by this line was counted. (H&E staining). C. Representative image of the application of thresholding to distinguish tissue (highlighted in green). The formula for calculating the Tissue Density (TD) is the following: TD=tissue area/(area of the lung (total or ROI))*100. D. Histological image of a cross section of a fetal pulmonary peripheral artery on which external (ED) and internal diameter (ID) were*

measured along the shortest axis (H&E staining). From these, the proportionate medial thickness (MT%) was calculated using the equation: MT%=(ED-ID)/ED x100.

For the evaluation of MT%, 10 random peripheric muscularized vessels with external diameter (ED) 100 μm, corresponding in rabbits to the pre- and intra-acinar arteries, were selected for each section. Their external (ED) and internal diameter (ID) along the shortest axis of the vessel were measured at 40x magnification (Figure 8 C) and MT% was calculated by applying the following formula: MT%=(ED-ID)/EDx100[77].This proportional parameter nullifies the effect of vasodilation, vasoconstriction, and tissue shrinkage.

3.4 Transcriptomic profiling

3.4.1 RNA Purification, Library Preparation and Sequencing

After collection, lungs were immediately placed in RNA Later (Sigma Aldrich, USA) and stored at -20°C. Samples were homogenized in QIAzol® Lysis Reagent. Total RNA was extracted with the miRNeasy Mini Kit protocol (QIAGEN, Germany), using an automated method (QIAcube: QIAGEN, Germany), adapted to include DNase I treatment. RNA concentration was measured using Qubit 4 fluorometer (Thermo Fisher Scientific, USA). RNA integrity was assessed checking the 2:1 ratio of 18S and 28S ribosomal RNA bands and RNA Integrity Number (RIN) by agarose gel electrophoresis and Bioanalyzer RNA 6000 Nano Kit (Agilent, USA), respectively. Lung-derived RNA was suitable for RNA-sequencing (RIN > 8). Libraries for massive parallel RNA sequencing were prepared using the QuantSeq FWD and Small RNASeq kits (Lexogen, Austria), and sequenced, in three different runs due to the high number of samples to be examined, with the Illumina

NexSeq500 platform, which generated at least 20 million reads for each sample, 96% of which, on average, could be mapped.

3.4.2 Bioinformatic analyses

Read quality analysis was performed with the FastQC tool and the adapters' sequences were trimmed with BBduk from the suite BBtools (http://jgi.doe.gov/data-and-tools/bb-tools/). RNA-seq reads were aligned on the rabbit genome (Oryctolagus cuniculus, OryCun2.0) with STAR[78] and gene counts were obtained with HTSeq-count[79],using the latest Ensembl available annotation on rabbit. A custom script, available upon request, was employed to account for reads mapping to unannotated 3' UTRs of protein coding genes (manuscript in preparation). Batch effect due to the different sequencing runs was removed using remove BatchEffect function in limma[80]package for R. Each sample count was related to the sample library size and transformed in CPM (Counts Per Million). Expressed genes were filtered using a threshold of 0.5 CPM in at least 3 samples. A Trimmed Mean of M values (TMM) normalization and then limma's voom function were applied. Differentially expressed genes (DEGs) were identified with the limma-voom tool (Bioconductor, R package). Genes were deemed to be differentially expressed if the absolute fold-change (FC) was > 2 and the adjusted p-value was ≤ 0.05.

3.4.3 Gene co-expression analysis

Modules of co-expressed genes were identified using the WGCNA package in R[81] (Langfelder & Horvath, 2008). This analysis was performed on data collected from fetal and term groups. Only genes with a minimum expression of 0.5 CPM in all samples of at least 3 out of the 4 developmental phases considered (pseudoglandular – canalicular – saccular – alveolar) were used for module construction. Modules were identified on a signed network using the blockwise. Modules function (WGCNA package in R) set at default parameters, excepting for the soft thresholding power set at

10, minimum module size set at 30, and merge CutHeight set at 0.25. Module Eigengenes were correlated with histological parameters using Pearson correlation. Pathway enrichment analysis was performed using Metascape software[82].Gene Ontology Biological Processes, KEGG Pathway, Reactome and Hallmark Gene Sets databases were used. Only terms with q-values ≤ 10-4 were considered significantly enriched. Heat maps were generated using Morpheus tool at https://software.broadinstitute.org/morpheus. Principal Component Analysis (PCA) was generated using scatterplot3D tools in R.

3.5 Transcriptomic comparison between rabbit and mouse lung development

An independent dataset from Beauchemin K.J. study[69] (GEO: GSE74243)) was used to compare mouse and rabbit lung developmental transcriptomic profiles. DEG lists were created using limma-voom tool in R, to compare expression profile at preterm and natural birth in both species. In particular, E18.5 vs P0 (mice) and F28 vs D31 (rabbits) comparisons were considered.

4 Results

4.1 Study design

Samples were collected at different lung developmental phases: pseudoglandular (P) (F20 n=4, F23 n=4), canalicular (C) (F25 n=3, F27 n=3), saccular (S) (F28 n=3, F29 n=3) and alveolar (A) (T31 n=6, T35 n=3, T37 n=4, and T42 n=3), for evaluating the histological and transcriptomic profiles of rabbit normal lung development. In addition, the prematurity impact was evaluated comparing gene expression and histological profile of preterm with term animals of equivalent gestational age (GA). Specifically, preterm animals maintained with 21% oxygen for 1 h, 3 and 7 days (P0 n=3, P3 n=3, and P7 n=3) were compared with fetal and term (F28, T31 and T35) samples.

4.2 Physiological rabbit lung development characterization

4.2.1 Lung tissue morphometry

The tissue morphology of normal lung development was characterized at different gestational ages that represent different phases of lung development from pseudoglandular to alveolar. Histological analysis highlighted in the pseudoglandular phase, the formation of primary lung buds and the beginning of branching morphogenesis processes. At time point F20 (Figure 9 A), the lung looked like a tubular gland, whereas in animals collected at F23 (Figure 9 B, C), end of the pseudoglandular phase – beginning of the canalicular phase, airway epithelial differentiation became visible. Some of the epithelial tubes at their distal end widened into airspaces covered by a more flattened epithelium,

in comparison to the conducting airways one. This distinction allowed the recognition of the acinus/ventilatory unit for the first time. During the canalicular stage the differentiation of prospective acini is accompanied by development of the capillary bed, the beginning of type I pneumocytes cell differentiation and the thinning of the mesenchymal tissues.

On F25 (Figure 9 D), all airway generations became greatly widened, elongated, and branched. Simultaneously there was a marked reduction of the pulmonary interstitial connective tissue. Each terminal bronchiole branched into 2 - 4 wide and straight acinar canals lined by cuboidal epithelial cells, some of which started to flatten and differentiate into type I pneumocytes. Vascularization of the surrounding mesenchymal tissue was progressively increased. Sections stained with Orcein demonstrated fine elastic fibers in inter-canalicular septa, arranged along the perimeter of the air spaces (Figure 9 F). At the end of canalicular phase, F27, (Figure 9 E) and the beginning of saccular stage, F28 (Figure 9 G), the terminal bronchioles branched out into several potential alveolar ducts ending in typical groups of enlarged air spaces (the terminal sacs). The terminal bronchioles were accompanied by thick-walled arterioles. The future airways appeared similar to “canaliculi” and this aspect gave the name at the stage of development. The mesenchymal tissue surrounding the terminal sacs condensed to form thick and highly cellular inter-saccular septa or primary septa that started to develop into secondary septa. In addition, during the transition from canalicular to saccular stage, the elastic fibers began to concentrate in the apical portion of the developing secondary crests. At the end of the canalicular stage most of the distal airways were formed, however during the saccular stage few terminal airways continued to develop. The saccular stage is an intermediate stage, between branching morphogenesis and alveolarization. We reported that the architecture of the lung parenchyma continued to develop in the animals collected during the transition from saccular (F29) to alveolar stage (T31) (F29, Figure 9 H-I and T31, Figure 9 J, L). In particular, we highlighted an increase in the number of secondary crest and alveoli that were signs of alveolarization process. After birth (T35, Figure 9 K; T 37, Figure 9 M, O; T42 Figure 9 N), the alveolarization process continued.

Septation process and the formation of new secondary septa was reported meanwhile the inter-alveolar septa become thinner. In parallel, due to the microvascular maturation, the two capillary layers formed a single -layered capillary network in a thin septa.

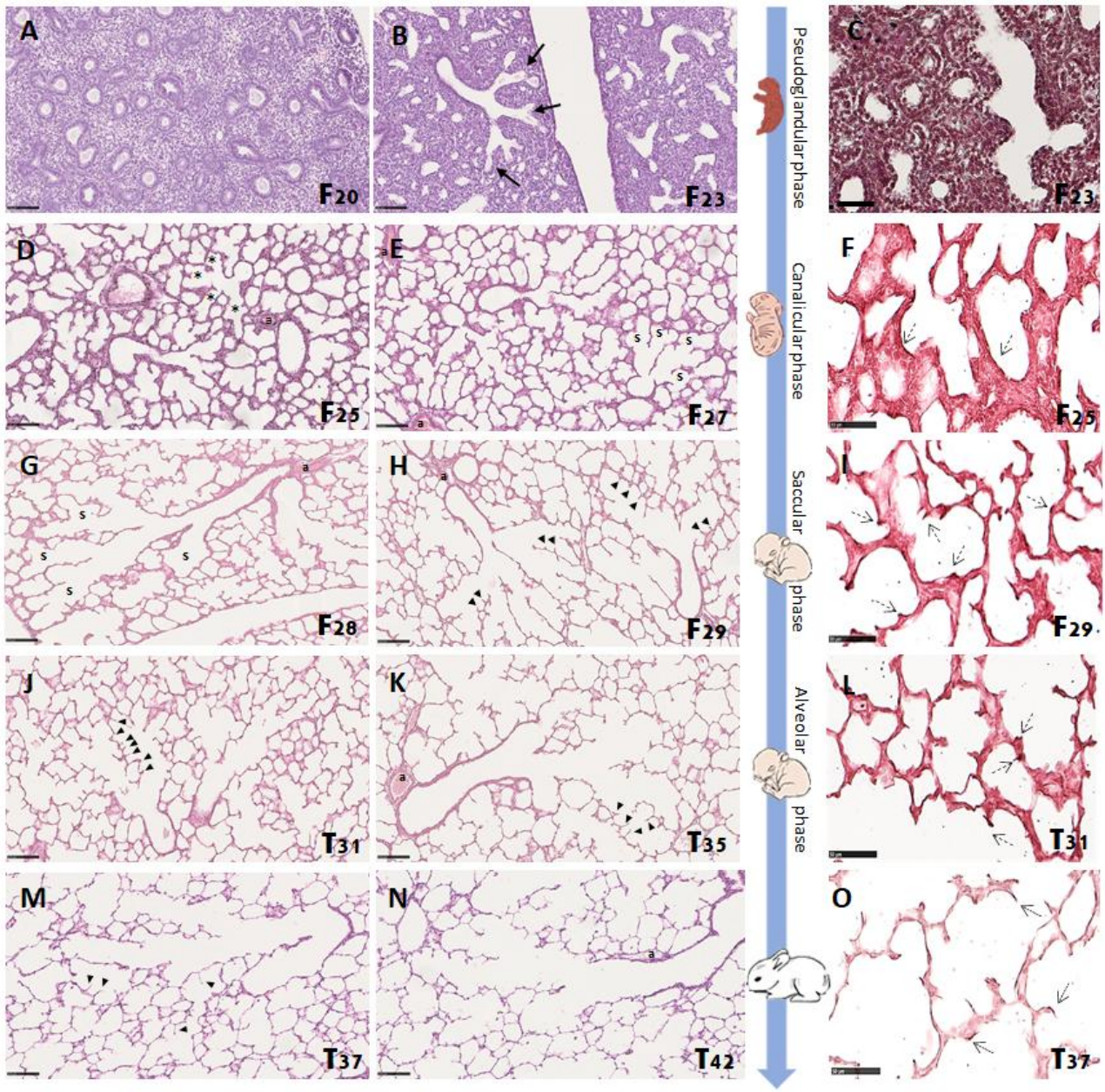

Figure 9. Histological and histomorphomtric characterization of the physiological rabbit lung development.

A-C. Representative images of the lung parenchyma during the pseudoglandular phase (the exact gestational age is reported on the images, F= fetal period, T post natal period; Term=31 days). Acinus/ventilatory unit (black arrows; A-B: H&E staining). TM staining (C). D-F. Representative images of the lung parenchyma during the canalicular and (G-I) saccular phases. Acinar canals (asteriscs) (a=pre-acinar arteriole) (H&E staining). (E, G; H&E staining). Terminal sacs, indicated with "s". Secondary crests (arrowheads; H&E staining). I. The elastic fibers (dotted arrows; Orcein staining). G-O. Representative images of the lung parenchyma during the alveolar phase. secondary crests (arrowhead). (J-K, M-N: H&E staining, L and O: Orcein staining).

The histological qualitative analysis was confirmed by the quantitative evaluation of the histomorphometric parameters: TD, RAC, and MT%. The progressive thinning of interalveolar septa and airspaces enlargement during lung development (Figure 10 A and B) was confirmed by a gradual reduction of the TD (Figure 10 D). In particular, we reported a significant decrease of TD values during the transition from the pseudo-glandular to the canalicular phase that remained stable, about 20%, until the alveolar phase. Whereases, the increase in alveoli number was confirmed by a significant increase in terms of RAC value (Figures 10 B and E). In parallel to the alveolarization process we confirmed also the progression of the angiogenesis process. We reported a MT% gradual decrease (Figures 10 C and F) from pseudoglandular to the alveolar phase that was a sign of the progressive thinning of the pre- and intra-acinar arterioles.

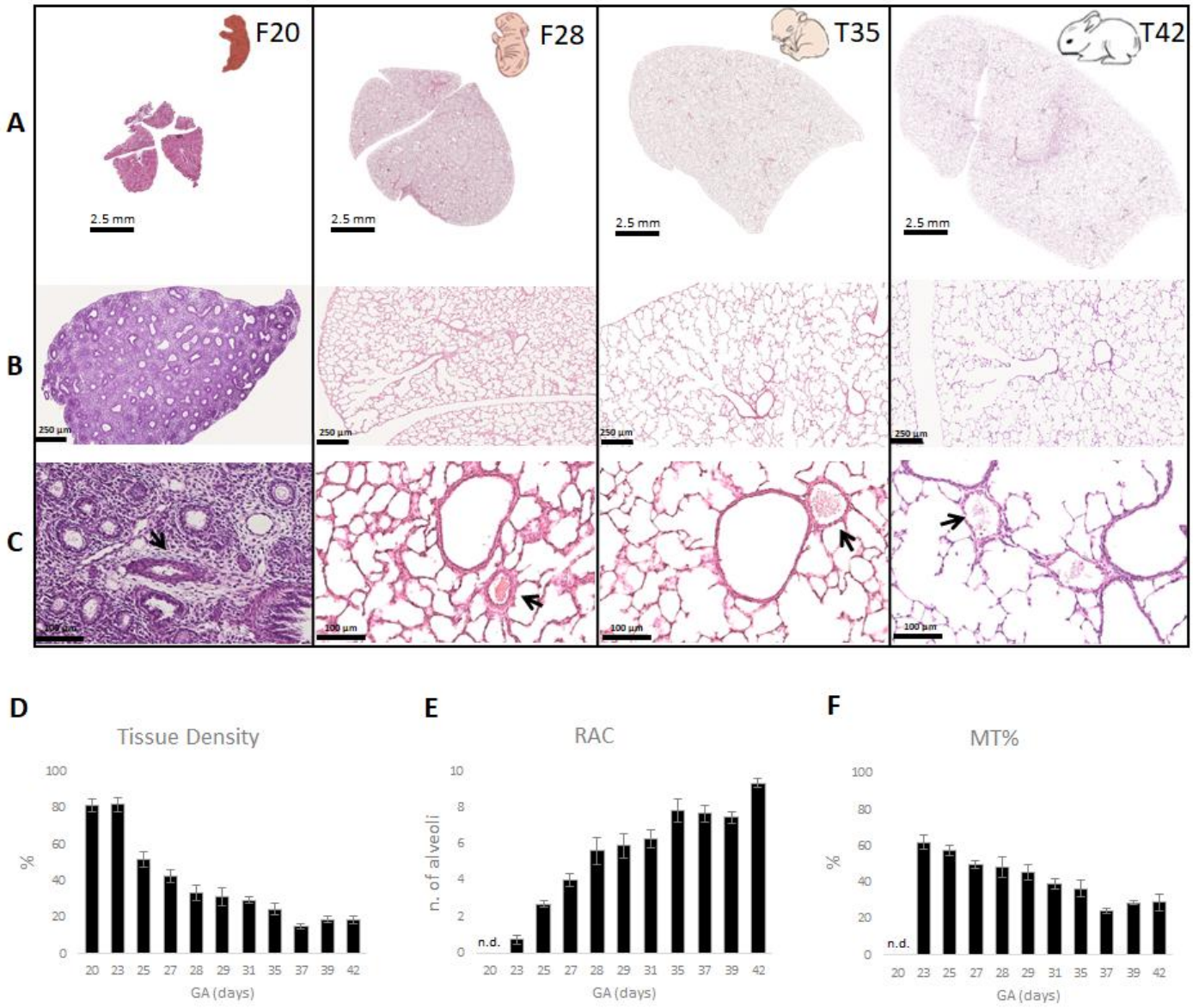

Figure 10. Histological and histomorphomtric characterization of the physiological rabbit lung development. H&E staining. A-B. Representative WSI (A) and microphotographs (B) of the lung parenchyma on F20 (pseudoglandular phase), F28 (saccular phase), T35 and T42 (alveolar phase). C. Representative pictures of the cross section of pre- and intra-acinar arteries (black arrows) on F20, F28, T35 and T42.D. Decrease of tissue density from fetal up to post-natal phases. E. Radial alveolar count (RAC) increase during rabbit lung development. F. Decrease of the medial thickness of pre- and intra-acinar arteries (MT%) parameter during rabbit lung development. Data are shown as mean ± S.E. n.d. = not detectable: due to the immaturity of the lung, the parameter is not evaluable because the morphological structures investigated are not present in sufficient number to perform the analysis. GA= gestational age.

4.2.2 Transcriptomic profiling

4.2.2.1 RNA isolation, library preparation and sequencing

Transcriptomic analysis was performed to characterize phase-related expression patterns during physiological lung development. RNA extracted was suitable for RNA-sequencing (RIN > 8). Three RNA-seq runs were performed due to the high number of samples considered. At least 20 million reads were sequenced and an average on 96% mapped reads was obtained. For normal lung development analysis, run 1 and 3 data were analyzed. After batch effect correction and TMM normalization, samples were filtered for lowly expressed genes: in the end 12506 protein-coding genes were identified, 11482 of which (92%) got an identified human orthologue. The global expression pattern was visualized using principal component analysis (PCA) (Figure 11 A). The PCA analysis showed that samples collected at the same lung developmental phase grouped together. Fetal samples clustered more tightly in the different time points compared to the term ones. The birth at term (T31), resulted the time point with the highest dispersion among replicates. Overall, these results suggested a progressive gene expression variation from fetal to term groups.

4.2.2.2 Phase-specific DEG analysis

Limma-voom analysis identified a total of 4160 genes as differentially expressed between different lung developmental phases/time points. The number of DEGs in each phase-comparison is reported in Figure 11B. As expected, the number of DEGs increased with the temporal distance between the two phases considered and the highest number of DEGs was identified between the most distant phases (P-A), in line with large changes in the transcriptomic profile occurring during lung development. Conversely, a lower number of DEGs was reported in the comparisons between phases that are chronologically close (P-C; C-S and S-A). The lowest DEG number was shown in the saccular vs alveolar (S-A) comparison.

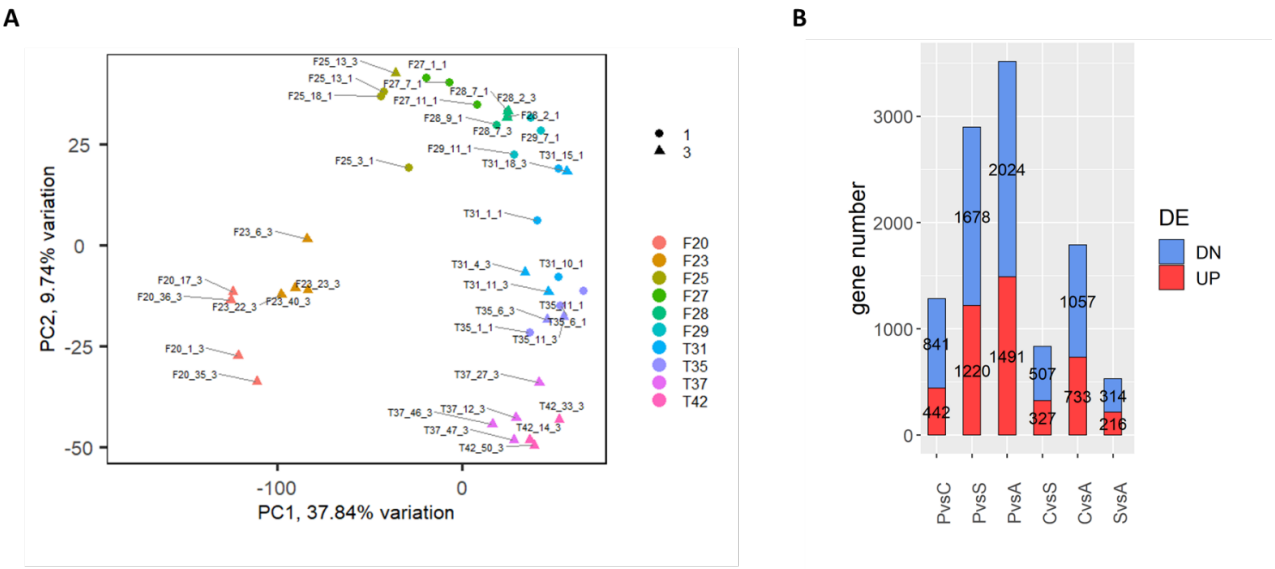

Figure 11. Transcriptomic characterization of physiological rabbit lung development, on fetal and term groups. A. Principal component analysis (PCA) showed specific clusters among samples of the same time point. B. Histogram representation of differentially expressed genes (DEGs) across time points comparing lung developmental phases (P=pseudoglandular, C=canalicular, S=saccular, and A=alveolar phases). Up-regulated genes are shown in red and down-regulated genes are shown in blue. The highest number of DEGs were identified in the P vs A phase comparison.

4.2.2.3 Time-dependent expression profile analysis

A network-based approach, WGCNA, was used to identify specific time-dependent transcriptional profiles and to integrate the results of DEGs analysis. The analysis identified 10 modules of co-expressed genes (Figure 12A). For each module, the expression profile was summarized in a representative profile as the module eigengene (ME) (Figure 12A). The first four modules accounted for about ¾ of all the analyzed genes. To facilitate biological interpretation, enrichment analysis was performed on genes belonging to each module to investigate processes involved in different phases of lung development (Figure 12B). Module 1 was characterized by a gene expression level that increased from saccular to alveolar phase (Figure 12A). As it accounts for more than 2500 genes, this module represents one fifth of the transcribed genes. Enrichment pathway analysis showed that several pathways critical for the latest fetal phases of lung development were included in module 1,

such as autophagy, morphogenesis of an epithelium, response to transforming growth factor-beta (TGF-β), angiogenesis, epithelium/endothelial cells development, and epithelium/endothelial cells migration processes. In addition, pathways that might be activated in response to natural birth, such as response to oxidative stress, complement cascade, and TNFA signaling via NFKB, were part of this module. Modules 2, 3, and 6 were characterized by an opposite trend, with high gene expression levels in the pseudoglandular phase that decreased during the later phases of lung development (Figure 12A). Cell cycle, embryo development, epithelium morphogenesis, collagen biosynthesis, mTOR signaling, RNA processing, oxidative phosphorylation, and WNT signaling pathways were enriched in these modules and were related to early embryonic morphogenesis. Indeed, almost 40% of genes belonging to these modules encoded for proteins with predicted nuclear localization. Gene expression levels in module 4 increased from birth to 11 postnatal days (Figure 12A). After term birth on 31st day of gestation, innate and adaptive immune response, angiogenesis and reactive oxygen species metabolic pathways were activated as reported in Figure 12B. Module 5 was characterized by an increase of gene expression levels from fetal to early alveolar phase (from F25 up to T35) with a decrease in the later part of the alveolar phase in T37 and T42 groups (Figure 3C). Autophagy and vesicle-mediated transport were the most representative pathways in this module. Module 7 and 8 reported a high gene expression level between canalicular and saccular phases (Figure 12A) and a low expression level in the alveolar phase whereas modules 9 and 10 were characterized by a low gene expression level in canalicular - saccular phases, and a high gene expression level in the later alveolar phase (Figure 12A). Module 7 displayed an enrichment in translation processes and oxidative phosphorylation, while the last three modules (8, 9 and 10), which accounted for a total of 504 genes, were not significantly enriched.

Figure 12. Time-dependent expression profile analysis A. Module eigengene (ME) heatmap represents each time-point sample from fetal up to post-natal phases. Median-normalized expression level is indicated on a low-to-high scale (blue–white–red). B. Results of pathway enrichment analysis on distinct modules of co-expressed genes. Representative terms significantly enriched in one or more modules are shown. Color saturation corresponds to enrichment significance (Log q-values).

WGNA analysis allowed to correlate each module with phenotypic traits associated to each time-point, like the histopathological parameters. Therefore, Pearson correlation between the MEs of each module and the histological parameters (RAC, TD, and MT%) was measured (Figure 13). Module 1 displayed the strongest correlation with one of the histological parameters, in particular it negatively correlated with TD (p-value 10^{-18}). In addition, Module 2 displayed the highest positive correlation with TD, p-value $3x10^{-12}$ whereases Modules 4 displayed the highest correlation with RAC (p-value $4x10^{-13}$).

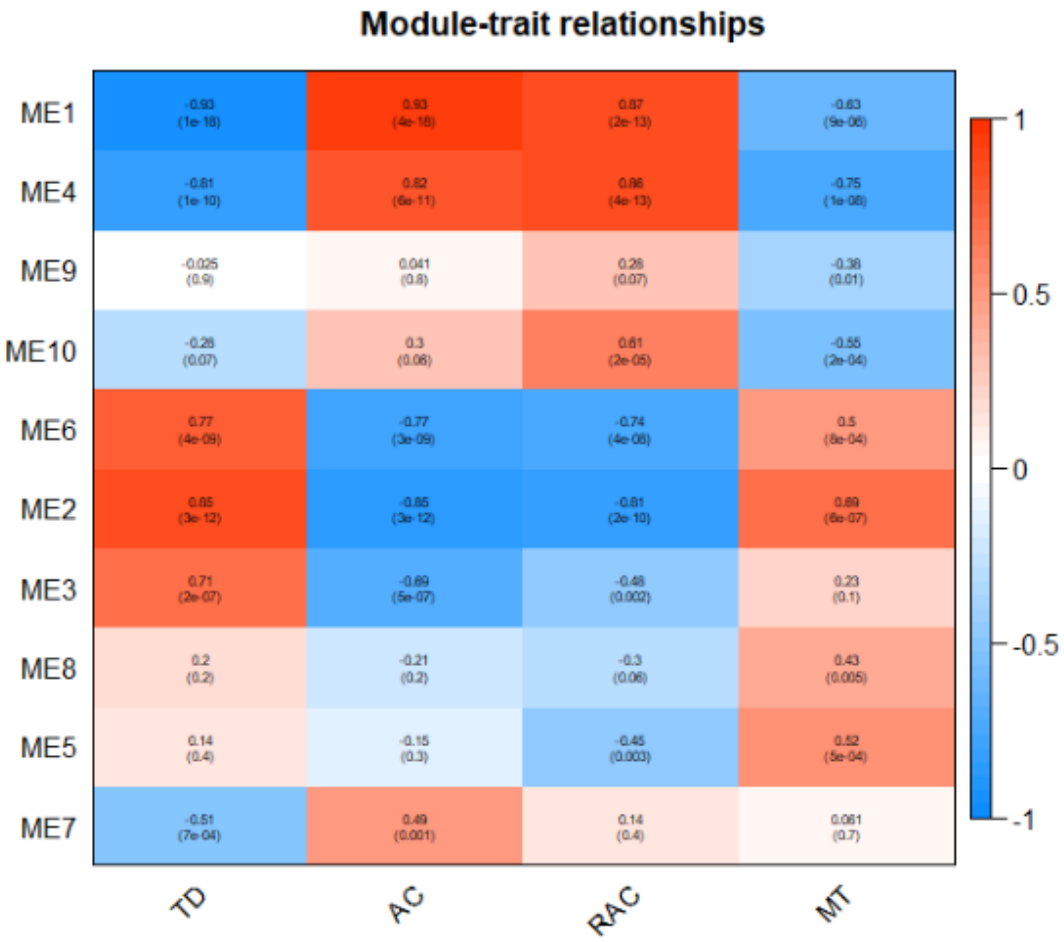

Figure 13 Transcriptomic and histological correlation.

4.3 Prematurity impact on rabbit lung development

In order to characterize the impact of the preterm birth on normal rabbit lung development we compared the transcriptomic and histological profile of samples collected at different time points. In particular we compared preterm animals born at 28th day of GA through a C-section procedure and maintained in customized chamber at 21% of O_2 for 1h(P0), 3 days (P3) and 7 days after birth (P7) with aged-matched animals birth at day 28 (T28), at term 31st day of GA (T31) and maintain with dams for four days (T35).

4.3.1 Histological analysis

Lung morphostructural and histomorphometric two-point comparison was analyzed between preterm (P3 and P7) and aged-matched animals (T31, and T35). The TD of both term and preterm animals decreased during the time course. Full-term pups showed significantly higher TD that premature ones 3 days after birth, however no significant difference was detected after 7 days. (Figure 14A and 14D).

The RAC showed comparable values in preterm and term animals at birth. The RAC values increased over time, always remaining slightly lower in preterm animals (Figure 14B and E).

Finally, the MT% parameter resulted significantly smaller in preterm pups in comparison to term animals (Figure 14C and F).

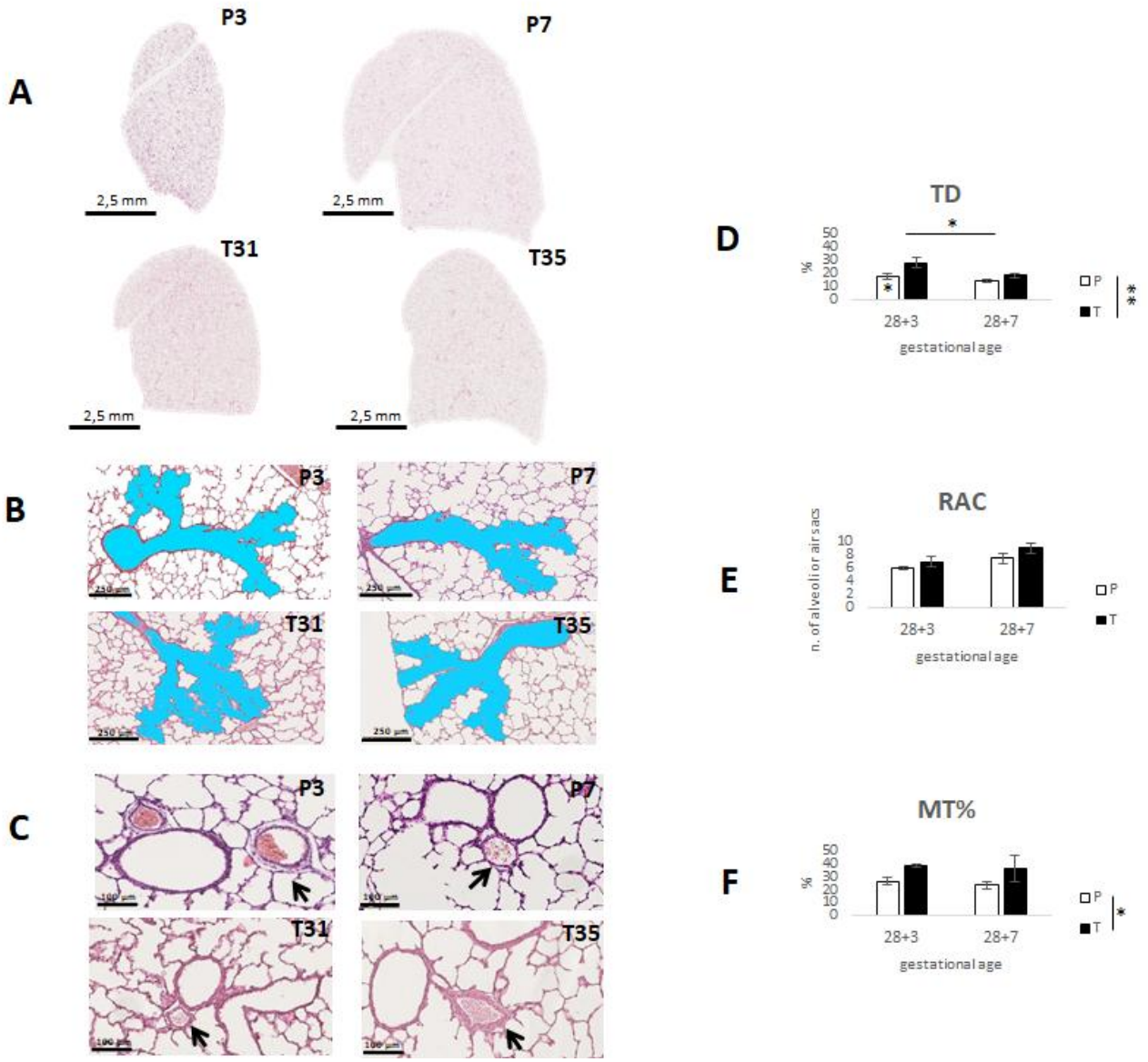

*Figure 14. Effects of prematurity on alveolar and vascular structure. Comparison between rabbit pups born on day 28 of gestation (P) and pups born at term (T). A. Representative whole slide images of the left lung cross section of P pups at 3 (P3) and 7 days (P7) after birth; moreover, of T pups at birth (T31), and 4 days after birth (T35). H&E staining. B. Representative microphotographs of lung parenchyma of P and T pups. Pulmonary acini are highlighted in blue. C. Representative pictures of the cross section of pre- and intra-acinar arteries of P and T pups. D. The tissue density (TD) is different between P and T pups 3 days after birth, but no differences are detected after 7 days. E. The radial alveolar count (RAC) is comparable in P and T pups both at 3 and 7 days after birth. F. Arterial medial thickness (MT%) is significantly smaller in P in comparison to T pups. Statistical analysis was performed using two-way ANOVA followed by Tukey's post hoc test, using birth condition (P or T) and gestational age (28+3 and 28+4 days) as factors. Asterisk within white bars indicates significant interactions, i.e. significant differences between P and T at a given time point. Asterisks above the horizontal lines indicate significant differences in the comparison between time points; asterisks near the vertical lines to the right of the legend indicate differences between P and T groups. *=p<0.05, **=p<0.01.*

4.3.2 Transcriptomic analysis

The impact of prematurity on rabbit lung physiological gene expression was evaluated comparing the transcriptomic profiles of preterm (P0, P3 and P7) and age-matched term pups (F28, T31 and T35) (Figure 15A). Several DEGs (62 in P0 vs F28, 51 in P3 vs T31, and 214 in P7 vs T35 comparisons, respectively) were identified using limma-voom tool. The up-regulated genes outnumbered down-regulated genes in all comparisons (71.7%-86.0% of total DEGs, Figure 15B). Nevertheless, when considering age-matched pups, genes up-regulated in the P7 vs T35 comparison could be due both to a decrease of gene expression during normal development or to an increase in pre-term pups. In addition, we identified sets of normal development- or preterm-specific DEGs, i.e. lists of genes whose expression levels significantly changed during normal lung development (F28 vs T35 comparison), but not in preterm animals (P0 vs P7 comparison), or vice-versa. The expression levels of the selected genes across all samples are reported in Figure 15C. Indeed, this longitudinal analysis allowed to distinguish, for example, genes whose expression specifically increase in pre-term pups (set 3 in Figure 15C) from those whose expression specifically decrease in normal development (set 2 in Figure 15C), which resulted both up-regulated in P7 vs T35 comparison. The four gene sets (genes up-regulated only in term or in preterm animals, plus genes down-regulated only in term or in preterm animals) were used for pathway enrichment analysis, together with the above mentioned age-matched DEGs. The most representative enriched processes are shown in Figure 15C. Pathway enrichment analysis revealed a prevalence of upregulated, immune system-related genes and pathways in the preterm animals in comparison to the age-matched term pups. The significance of the above pathways increased as a function of post-natal time, i.e., from P3 vs T31 to P7 vs D35 comparisons, and moreover were specifically up-regulated only in preterm pups, i.e. P7 vs P0 comparison (gene set 3 Figure 15C). P0 vs F28 up-regulated genes were significantly enriched in TNF-responsive, NF-kB-regulated genes. Genes characterized by a significantly decreased expression during normal development, but not dysregulated in preterm pups were enriched in

hypoxia pathway-related genes, whereas genes involved in cell adhesion, heme metabolism and epithelial-mesenchymal transition processes were exclusively upregulated in term animals (gene set 1, T35 vs F28 comparison).

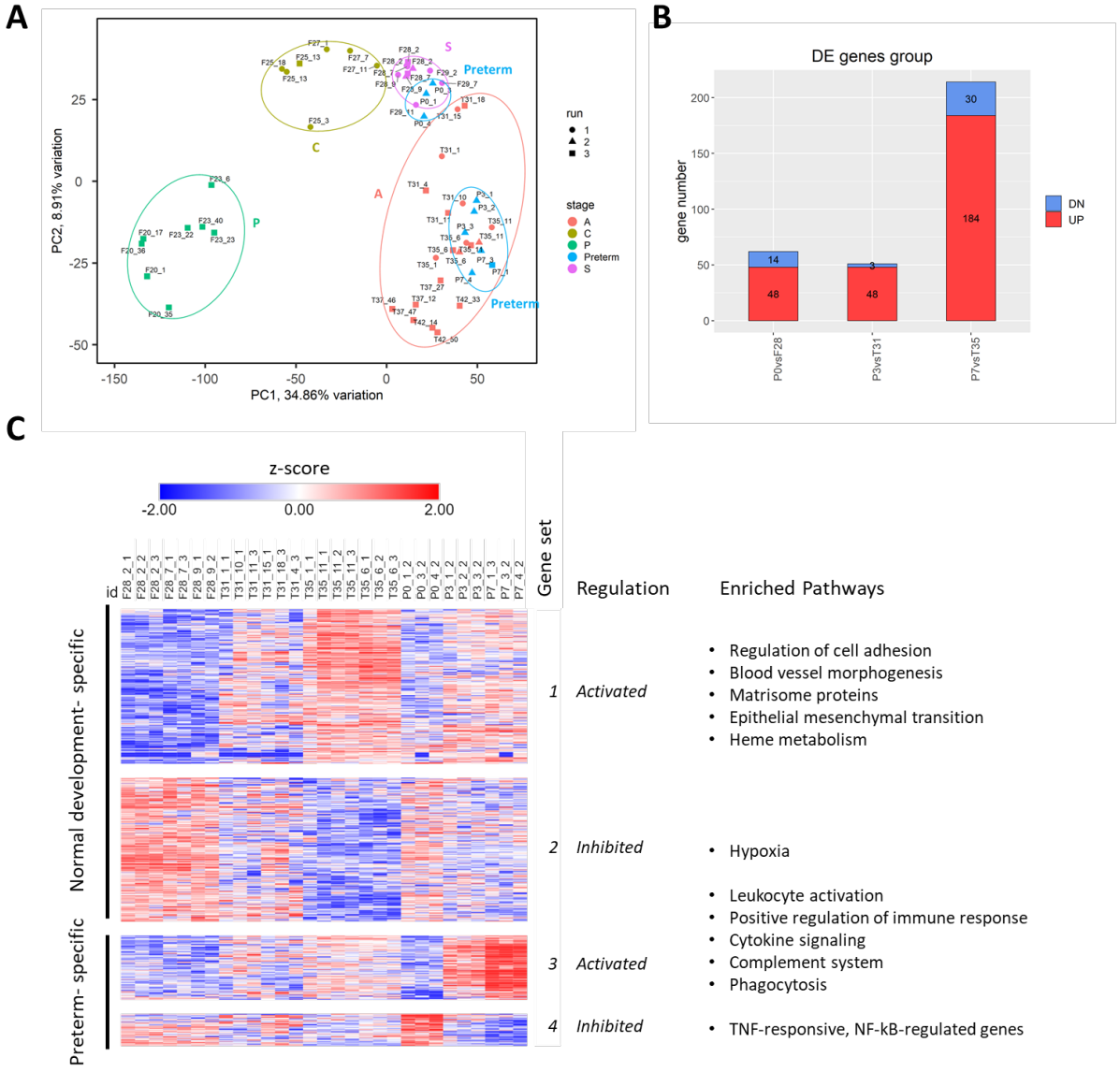

Figure 15. Prematurity impact on physiological rabbit lung development A. Principal component analysis (PCA) shows preterm pups clustering closely to, yet well separated from, term pups of the same gestational age. B. Number of differentially expressed genes derived from comparisons between preterm groups and age-matched term groups. Up-regulated and downregulated genes are shown in red and blue, respectively. C. Heatmap representing expression levels of normal development- or preterm-specific genes (i.e. selected because showing significant expression variations only in term animals and not in preterm animals or vice-versa). Z-score-normalized expression level is indicated on a low-to-high scale (blue–white–red). Representative terms resulting from pathway enrichment analysis, performed with Metascape software, are reported.

4.4 Transcriptomic comparison between rabbit and mice lung development

Rodents are the most used animals for preclinical study on BPD. In the BPD model, rodent pups born at term in the saccular stage. At this stage the lungs are structurally immature but functionally mature because born at term and they are fully capable of extrauterine survival. This aspect significantly reduces their translational power as BPD model. On the contrary in the preterm rabbit BPD model pups born prematurely in the saccular phase. They have structurally but also functionally immature lungs, they are not fully capable of extrauterine survival like preterm neonates. In order to demonstrate the translational power of the preterm rabbit as BPD model, we compared rabbit data with currently literature-available data from a preclinical transcriptomic study on lung development in mice. In order to perform the comparison analysis, DEG lists were created starting from the independent dataset on mice normal lung development (as described in material and methods section). Lung developmental time points and phases in mice and rabbits are shown in Figure 16A. DEG lists were created, comparing time points of preterm and term birth in rabbit (F28-T31) and mice (E18.5-P0). Pathways enrichment analysis was applied on identified DEG lists. In particular, we considered pathways up-regulated at term (T31 rabbit – P0 mouse) and preterm (F28 rabbit – E18.5 mouse) birth in both species. The results suggested that the expression profile at preterm and term birth in both species was similar. Organ development characteristic pathways such as cell cycle, regulation of cell division, cell cycle checkpoint, and mitotic processes were up-regulated in mice and rabbits at preterm birth. Moreover, Log q-values of each pathway were comparable between the species (Figure 16B). In addition, DEG lists analyzed at term birth in both species were enriched in angiogenesis, vasculature development, blood vessel development, humoral immune system, leukocyte migration, and TNFα via NFKB (Figure 16C). However, if we compare the starting point of the two BPD models, term mice and preterm rabbit, we reported a different expression profile. In particular term

mice in comparison to preterm rabbit showed an upregulation of pathways related to blood vessel development and activation of immune systems confirming that they are fully capable of extrauterine survival. No common enriched pathway emerged from the comparison between preterm rabbits and term mice This result supports the high translational power of preterm rabbit as suitable animal model for studying the dysregulation of lung development-related pathways, leading to BPD.

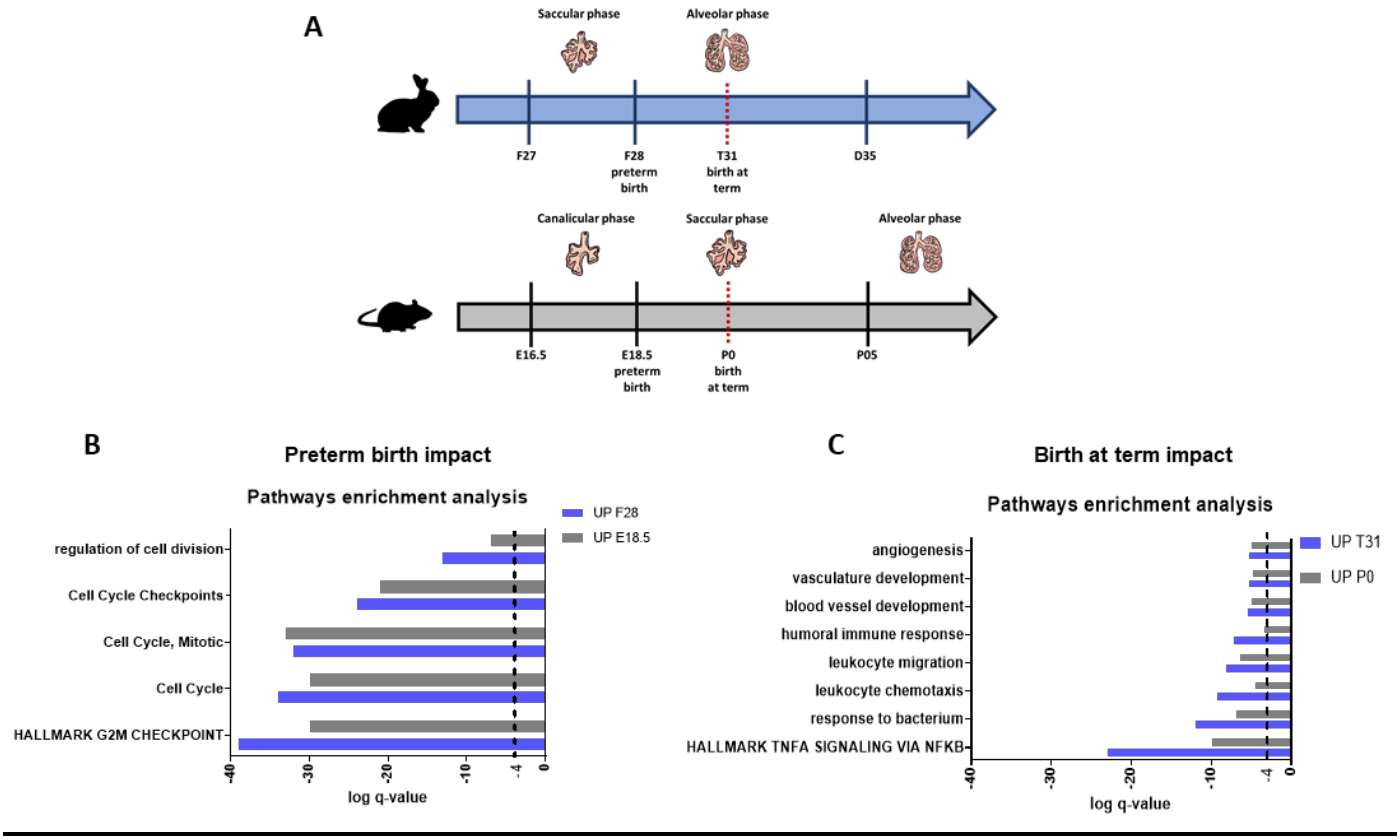

Figure 16: Developmental gene expression comparison between rabbits and mice. A. Comparison between rabbit and mouse physiological lung development. Rabbits are born at term (T31) in the alveolar phase, whereas mice are born at term (P0) in the saccular phase. Mice enter in the alveolar phase only 4-5 days after birth. B. Up-regulated pathways in rabbits (blue line) and mice (grey line) at preterm birth (F28 and E18.5 time points, respectively). C. Up-regulated pathways in rabbits (blue line) and mice (grey line) at term birth (T31 and P0 time points, respectively). The identification of processes enrichment for each comparison was performed using the Metascape software. Only processes with q-values ≤ 10-4 were considered significantly enriched.

5 CONCLUSION

Suitable animal models can improve knowledge on the molecular and signaling pathways that control the normal lung development. Preclinical research that focuses on the identification of pathways that are involved in in-utero lung development and disrupted by respiratory disorders and pre-term birth, could lead to novel therapeutic strategies for BPD, the most common respiratory morbidity in preterm neonates. In this regard the hyperoxia-exposed preterm rabbit model could represent a valuable lab preclinical tool for mimicking the clinical BPD phenotype for testing new pharmacological treatments. However, the molecular characterization of rabbit lung development is lacking. In our study, we reported a comprehensive characterization of the normal rabbit lung development and the impact of the prematurity on the molecular pathways that regulate the postnatal lung architecture. The possibility to investigate the premature delivery, the common denominator in the heterogeneous spectrum of human BPD, allows us to show the translational advantage to use preterm animals for BPD research. In order to obtain a full picture of the lung development process we collected samples that span along four lung developmental stages: pseudoglandular (F20-F23), canalicular (F25 – F27), saccular (F28 – F29) and alveolar (T31 – T 35 – T37- T42) phases. Histological and transcriptomic analysis were performed to investigate the biomolecular processes that govern lung development. A branching morphogenesis process was reported starting from pseudoglandular (F20-F23) to the first part of saccular stage (F27) characterized by airway epithelial differentiation and formation of pre-alveolate saccules. In parallel, the alveolar epithelium comes into close contact with the mesenchymal capillary network in order to form the first form of future air–blood barriers. The saccular stage (F28 -F29) represents an intermediate step, the transition from branching morphogenesis to the alveolarization process. A relevant increase of alveoli numbers concomitant to TD decrease was reported starting from saccular phase (Figure 10), sign of a marked reduction of the pulmonary interstitial connective tissue and respiratory tree development[83,84]. In the alveolar phase, from birth to post-natal day 11, the number of secondary crests and alveoli increased. Air-blood barrier

thickness progressively decreased, as a thin air-blood barrier is crucial for effective gas exchange between air and blood[15,83–86] (Figure 9-10). The timing of lung maturation is controlled precisely by complex genetic and pathway programs[15,34] . In our study, transcriptomic results demonstrated a specific developmental pattern from pseudoglandular to alveolar phase. The PCA The PCA (Figure 11) analysis showed that samples collected at the same lung developmental phase grouped together. Fetal samples clustered more tightly among the different time points compared to the term ones. These differences might be related to the fact that term animals were naturally delivered at term, so the GA was not exactly the same among samples. On the contrary, preterm pups were delivered through a planned C-section so the variation among the samples collected at the same GA was limited. DEGs analysis between phases underlined different genes and consequently different pathways involved from pseudoglandular up to alveolar phases. It is worth to mention, that CvsS and SvsA had a lower number of DEGs compared to the other comparisons (Figure 11), implying that the saccular phase behaves as a transition step between canalicular and alveolar phases[15,87,88] .To describe the gene expression pattern and pathways involved in lung development we applied the WGCNA analysis on modules of co-expressed genes. WGCNA has been recently used to characterize and identify key biomarkers involved in several pathologies such as BPD[89–91].Pathway enrichment analysis on co-expressed genes modules identified several patterns that are involved in the normal lung development (Figure 12). Our results confirmed the literature data: cell proliferation characterized early lung development, highlighting lung responses to a nonsterile oxygen-rich ambient environment exposure and the important role of lipid (surfactant) metabolism in lung development. Cell cycle, embryo development, cell morphogenesis, RNA splicing, and translation pathways were upregulated in the first developmental phases, sign of organ expansion and early embryonic morphogenesis processes. Autophagy, FOXO-mediated transcription, TGFβ response, and epithelium/endothelium development pathways were upregulated from saccular (F28) up to alveolar phases (T42), essential during lung development, to create the organ and specialize it from the first hint up to a complex organ[15,67,92–94 95–98].Lipids metabolism increased in late pseudoglandular and saccular phases. This

might be required to support surfactant metabolism[83,99].Surfactant proteins are essential to maintain the structure and homeostasis of the lungs, and to avoid alveoli collapse[100]. Prior to birth, surfactant production and innate immune responses are critical and connected processes that positively influence lung maturation necessary for respiration and survival after birth. Our results highlighted an up regulation of the immune system pathway, response to oxidative stress, complement, and TNFA signaling via NFKB pathways in the transitional phase between saccular and alveolar stage. Initiation of breathing immediately after birth activated critical metabolic and cardiorespiratory changes[101]demonstrated by an upregulation of Reactive oxygen species (ROS) metabolic process and VEGF signaling. Both processes are critical in creating the vasculature in utero and after birth[98,102,103] . Positive regulation of cell migration and tissue morphogenesis processes were upregulated in the late alveolar developments. Our data were limited to 11 days after birth, however several studies reported that alveolarization was not related only to the perinatal period, but it continues during childhood and adolescence in human[85,104,105] .

Premature birth leads to several neonatal diseases such as BPD, interrupting the physiological lung development[106].The causes of preterm birth are associated with several factors such as maternal factors, genetic predisposition, C-section, intrauterine infection, fetal malformation, and multiple gestations[107–109].In our rabbit model we mimicked the prematurity insult only through C-section performed at day 28 of gestation in the saccular phase. Other relevant factors associated with preterm birth, such as prenatal infection have not been implemented yet. Salaets et al. have already investigated how prematurity affects lung structure and function in neonatal rabbits born at 28 days of GA[110].They observed after 7 days of life (P7) an increase in tissue damping, tissue elastance and resistance, and a decrease in dynamic compliance in preterm animals compared to the term ones. Regarding histological analysis, the authors showed that P7 preterm rabbits were comparable to term pups on four post-natal days (T35), indicating an, at least initial, continued postnatal lung development from saccular to alveolar phases regardless of premature delivery. Our histological results were in line with these findings (Figure 14) . However, our study for the first time

characterized the prematurity impact on the biomolecular process of the normal rabbit lung development. The prematurity impact was evaluated comparing transcriptomic profile of preterm animals birth at 28th day of gestation and maintained at 21% oxygen for 1 h, 3 and 7 days (P0, P3, and P7) with fetal (F28) animals born at 28th day of gestation and sacrificed before the first breath, and animal born at term at 31st day of gestation (T31) and maintained with dams for 4 days (T35).

Several DEGs were identified comparing transcriptomic profiles of preterm and age-matched pups (Figure 15). In particular, we performed a longitudinal analysis that identified genes whose expression specifically changed during normal lung development (F28 vs T35 comparison), but not in preterm animals (P0 vs P7 comparison), or vice-versa (Figure 15). Our results underlined a higher immune system activation in preterm rabbits from P0 up to P7 compared to age-matched term animals. Prior to birth, innate immune responses and surfactant production are critical and connected processes that positively influence lung maturation necessary for respiration and survival after birth. In addition, the antioxidant defense enzymes, which mature in parallel with the surfactant system, play an important role to prepare the fetus for its pulmonary adaptation at term birth. The lack of this preparation in the preterm neonate, requires endogenous adaptive strategies. Our results are in accordance with other scientific literature showing a delay in the immune system activation and ROS metabolic process in preterm rabbits in comparison with the age-matched term animals[36]. Nguyen et al. studied the delay of systemic immunity development in preterm vs near-term pigs. They demonstrated that systemic immunity follows a distinct developmental trajectory after preterm birth, confirming that the immature immune system in preterm neonates adapts after birth, and it is influenced by various factors in the postnatal period (external environment, variable antibiotic treatment, and impaired organ function)[36]. DEGs analysis on our data showed that heme metabolism pathway is only activated in term animals. Heme metabolism is linked to ROS and oxidative stress pathways[113]. ROS susceptibility has been observed in preterm babies[37,111,112].Moreover, hypoxia/reoxygenation episodes in early life could sustain a proinflammatory cascade as we reported in our analysis[114] .The only upregulated pathway in preterm animals is the hypoxia one. Several studies demonstrated that

preterm babies have high intermittent hypoxic episodes as a consequence of immature respiratory control. Overall, these results confirmed that prematurity has an impact on the rabbit physiologic lung development.

Preterm rabbit pups as premature neonates are not structurally and functionally prepared to extrauterine life at birth. On the contrary, mice and rats, the most used lab animal species to mimic chronic lung disease as BPD are well known to possess adaptive mechanisms to experience extra uterine life with structurally preterm lungs[53].At term, rodents are functionally in the saccular phase of lung development, which mimic morphologically human premature infants at 28-30 weeks gestation. This means that they could be good models to study alveolarization, but not necessarily the transition of the canalicular to saccular stage as occurring in human preterm babies developing BPD. This aspect significantly reduces their translational power as BPD models. On the contrary in the preterm rabbit BPD model, pups have structurally but also functionally immature lungs. They are not ready for of extrauterine life like preterm neonates. In order to demonstrate this theoretical difference in terms of translational power between preterm rabbit and term rodents as BPD models, we compared our rabbit transcriptomic data with literature-available data from a preclinical transcriptomic study on mouse lung development. Beauchemin and colleagues performed indeed a study on molecular characterization of mouse lung development along 26 time points from embryonic GA 9.5 up to post-natal day 56 in three common inbred strains of mice, analyzing pre- and post-natal processes[69] .To date, a comparison between developmental transcriptomic data on rabbits and mice has not been described in the literature. We compared the expression profile of preterm and term birth in rabbit (F28-T31) and mice (E18.5-P0). In particular, we considered pathways up-regulated at term (T31 rabbit – P0 mice) and preterm (F28 rabbit – E18.5 mice) birth in both species.

Organ development characteristic pathways such as cell cycle, regulation of cell division, cell cycle checkpoint, and mitotic processes were up-regulated in mice and rabbits at preterm birth (Figure 16). Whereas term animals in both species were enriched in angiogenesis, vasculature development, blood

vessel development, humoral immune system, leukocyte migration, and TNFα via NFKB. These results highlighted that physiological birth in both species activated common pathways despite their different lung developmental phases[52]. Furthermore, there were not common pathways between preterm rabbits (F28) and term mice (P0), the starting points of the two BPD models. In particular term mice showed an upregulation of pathways related to blood vessel development and activation of immune systems confirming that they are fully capable of extrauterine survival. On the contrary preterm rabbit showed an upregulation of pathways related to prematurity such as cell cycle and regulation of cell division. This result confirms for the first time the high translational power of preterm rabbit in comparison to term mouse as suitable animal model for studying the dysregulation of lung development-related pathways, leading to BPD. In conclusion, we characterized in depth the histological and transcriptomic profile of the rabbit normal lung development, and the impact of the prematurity on the molecular pathways that regulate the postnatal lung structure. Moreover, we demonstrated the high translational power of rabbit in comparison to mouse as BPD preclinical model.

It must be acknowledged that this study has some limitations. First of all, in order to demonstrate the translational power of the preterm rabbit as BPD model we did not compare our data with data on human physiological lung development. Unfortunately, due to ethical issues, transcriptomic studies on human lung development are strongly limited to the early developmental phases, so in the literature dataset on omics analysis applied to human samples collected during the later phases of lung development are not reported. Moreover, as mentioned above, our preterm model did not report prenatal insults that in human could stimulate preterm birth[107–109].Pre-eclampsia, chorioamnionitis, maternal smoking, and genetic predisposition increase the risk of preterm birth[115–117] ,affecting lung development in utero and after birth.

The data obtained from this study open a wide perspective window to future research. We could use this dataset on normal lung development to understand how postnatal factor such as hyperoxia can

impact on lung development. Jiménez and colleagues showed a development arrest with a BPD-like phenotype in the preterm rabbit exposed to hyperoxia, already at day 5[63]. To this end, it would be valuable to discriminate prematurity and hyperoxia contributions on physiological lung development disruption assessing genes and pathways that play a key role in the BPD development process.

6 REFERENCES

1. M. G. T. Moore, K. L. V. P. *The Developing Human. Clinically Oriented Embryology, 9th ed. Saunders*. (Elsiever, 2013).
2. Pereda, J., Sulz, L., San Martin, S. & Godoy-Guzmán, C. The human lung during the embryonic period: vasculogenesis and primitive erythroblasts circulation. *Journal of Anatomy* **222**, 487–494 (2013).
3. Wu, S. & Savani, R. C. Molecular Bases for Lung Development, Injury, and Repair. in *The Newborn Lung* 3–29 (Elsevier, 2019). doi:10.1016/B978-0-323-54605-8.00001-5.
4. Thébaud, B. *et al.* Bronchopulmonary dysplasia. *Nature Reviews Disease Primers* vol. 5 (2019).
5. Burri, P. H. & Tarek, M. R. A novel mechanism of capillary growth in the rat pulmonary microcirculation. *The Anatomical Record* **228**, 35–45 (1990).
6. Burri, P. H. Structural Aspects of Postnatal Lung Development – Alveolar Formation and Growth. *Neonatology* **89**, 313–322 (2006).
7. Warburton, D. *et al.* Lung Organogenesis. in 73–158 (2010). doi:10.1016/S0070-2153(10)90003-3.
8. Iliodromiti, Z. *et al.* Acute lung injury in preterm fetuses and neonates: mechanisms and molecular pathways. *The Journal of Maternal-Fetal & Neonatal Medicine* **26**, 1696–1704 (2013).
9. MASON, R. J. Biology of alveolar type II cells. *Respirology* **11**, S12–S15 (2006).
10. Joshi, S. & Kotecha, S. Lung growth and development. *Early Human Development* **83**, 789–794 (2007).
11. Sardesai, S., Biniwale, M., Wertheimer, F., Garingo, A. & Ramanathan, R. Evolution of surfactant therapy for respiratory distress syndrome: past, present, and future. *Pediatric Research* **81**, 240–248 (2017).
12. M. Rosenthal and A. Bush. The growing lung: normal development, and the long-term effects of pre- and postnatal insults. in 1–24 (Eur. Respir. Monogr, 2002).
13. Fraga, M. V. & Guttentag, S. Lung Development. in *Avery's Diseases of the Newborn* 571–583 (Elsevier, 2012). doi:10.1016/B978-1-4377-0134-0.10042-3.
14. Lewin, G. & Hurtt, M. E. Pre- and Postnatal Lung Development: An Updated Species Comparison. *Birth Defects Research* vol. 109 1519–1539 (2017).
15. Alan H. Jobe. *Fetal and Neonatal Lung Development*. (Cambridge University Press, 2016). doi:10.1017/CBO9781139680349.
16. Lewin, G. & Hurtt, M. E. Pre- and Postnatal Lung Development: An Updated Species Comparison. *Birth Defects Research* **109**, 1519–1539 (2017).
17. Shifley, E. T., Kenny, A. P., Rankin, S. A. & Zorn, A. M. Prolonged FGF signaling is necessary for lung and liver induction in Xenopus. *BMC Developmental Biology* **12**, 27 (2012).
18. Serls, A. E., Doherty, S., Parvatiyar, P., Wells, J. M. & Deutsch, G. H. Different thresholds of fibroblast growth factors pattern the ventral foregut into liver and lung. *Development* **132**, 35–47 (2005).

19. Wang, J. H. *et al.* Retinoic acid is a key regulatory switch determining the difference between lung and thyroid fates in Xenopus laevis. *BMC Developmental Biology* **11**, 75 (2011).

20. Hameed, A., Azhar Sherkheli, M., Hussain, A. & Ul-haq, R. Molecular and Physiological Determinants of Pulmonary Developmental Biology: a Review. *American Journal of Biomedical Research* **1**, 13–24 (2013).

21. Roth-Kleiner, M. & Post, M. Genetic Control of Lung Development. *Neonatology* **84**, 83–88 (2003).

22. Morrisey, E. E. & Hogan, B. L. M. Preparing for the First Breath: Genetic and Cellular Mechanisms in Lung Development. *Developmental Cell* vol. 18 8–23 (2010).

23. Maeda, Y., Davé, V. & Whitsett, J. A. Transcriptional Control of Lung Morphogenesis. *Physiological Reviews* **87**, 219–244 (2007).

24. Ornitz, D. M. & Yin, Y. Signaling Networks Regulating Development of the Lower Respiratory Tract. *Cold Spring Harbor Perspectives in Biology* **4**, a008318–a008318 (2012).

25. Boström, H. *et al.* PDGF-A Signaling Is a Critical Event in Lung Alveolar Myofibroblast Development and Alveogenesis. *Cell* **85**, 863–873 (1996).

26. Healy AM, M. L. Z. X. F. H. C. W. VEGF is deposited in the subepithelial matrix at the leading edge of branching airways and stimulates neovascularization in the murine embryonic lung. *Anatomists* **219(3):341-352**, (2000).

27. World Health Organization “Preterm birth.” *https://www.who.int/en/news-room/fact-sheets/detail/preterm-birth.* (2018).

28. Glass, H. C. *et al.* Outcomes for extremely premature infants. *Anesthesia and Analgesia* **120**, 1337–1351 (2015).

29. Hallman, M., Hallman, M. & Saarela, T. *62.1 Introduction Respiratory Distress Syndrome: Predisposing Factors, Pathophysiology and Diagnosis*.

30. Bahadue, F. L. & Soll, R. Early versus delayed selective surfactant treatment for neonatal respiratory distress syndrome. *Cochrane Database of Systematic Reviews* (2012) doi:10.1002/14651858.CD001456.pub2.

31. Glaser, K., Speer, C. P. & Wright, C. J. Fine Tuning Non-invasive Respiratory Support to Prevent Lung Injury in the Extremely Premature Infant. *Frontiers in Pediatrics* **7**, (2020).

32. Siffel, C., Kistler, K. D., Lewis, J. F. M. & Sarda, S. P. Global incidence of bronchopulmonary dysplasia among extremely preterm infants: a systematic literature review. *The Journal of Maternal-Fetal & Neonatal Medicine* **34**, 1721–1731 (2021).

33. Gibbons, J. T. D., Wilson, A. C. & Simpson, S. J. Predicting Lung Health Trajectories for Survivors of Preterm Birth. *Frontiers in Pediatrics* **8**, (2020).

34. Xu, Y. *et al.* Transcriptional programs controlling perinatal lung maturation. *PLoS ONE* **7**, (2012).

35. Bartman, C. M., Awari, D. W., Pabelick, C. M. & Prakash, Y. S. Intermittent Hypoxia-Hyperoxia and Oxidative Stress in Developing Human Airway Smooth Muscle. *Antioxidants* **10**, 1400 (2021).

36. Nguyen, D. N. *et al.* Delayed development of systemic immunity in preterm pigs as a model for preterm infants. *Scientific Reports* **6**, 36816 (2016).

37. Ozsurekci, Y. & Aykac, K. Oxidative Stress Related Diseases in Newborns. *Oxidative Medicine and Cellular Longevity* vol. 2016 (2016).

38. Martin, R. J., Wang, K., Köroğlu, Ö., di Fiore, J. & Kc, P. Intermittent Hypoxic Episodes in Preterm Infants: Do They Matter? *Neonatology* **100**, 303–310 (2011).

39. Gibbons, J. T. D., Wilson, A. C. & Simpson, S. J. Predicting Lung Health Trajectories for Survivors of Preterm Birth. *Frontiers in Pediatrics* vol. 8 (2020).

40. Abman, S. H., Bancalari, E. & Jobe, A. The Evolution of Bronchopulmonary Dysplasia after 50 Years. *American Journal of Respiratory and Critical Care Medicine* **195**, 421–424 (2017).

41. Bhandari, V. *Bronchopulmonary Dysplasia.* (2016).

42. Jensen, E. A. & Wright, C. J. Bronchopulmonary Dysplasia: The Ongoing Search for One Definition to Rule Them All. *Journal of Pediatrics* vol. 197 8–10 (2018).

43. Bhandari, A. & Bhandari, V. *PATHOGENESIS, PATHOLOGY AND PATHOPHYSIOLOGY OF PULMONARY SEQUELAE OF BRONCHOPULMONARY DYSPLASIA IN PREMATURE INFANTS*. *Frontiers in Bioscience* vol. 8 (2003).

44. Shahzad, T., Radajewski, S., Chao, C.-M., Bellusci, S. & Ehrhardt, H. Pathogenesis of bronchopulmonary dysplasia: when inflammation meets organ development. *Molecular and Cellular Pediatrics* **3**, (2016).

45. Jobe, A. H. *The New BPD*. http://neoreviews.aappublications.org/.

46. Fanni, D. *et al.* Bronchopulmonary dysplasia: understanding of the underlying pathological mechanisms The role of the clinical pathological dialogue in problem solving How to cite. *Proceedings Journal of Pediatric and Neonatal Individualized Medicine* • **3**, 30259 (2014).

47. Jobe, A. H. & Steinhorn, R. Can We Define Bronchopulmonary Dysplasia? *Journal of Pediatrics* **188**, 19–23 (2017).

48. Steinhorn, R. *et al.* Chronic Pulmonary Insufficiency of Prematurity: Developing Optimal Endpoints for Drug Development. *Journal of Pediatrics* **191**, 15-21.e1 (2017).

49. Higgins, R. D. *et al.* Bronchopulmonary Dysplasia: Executive Summary of a Workshop. in *Journal of Pediatrics* vol. 197 300–308 (Mosby Inc., 2018).

50. Hilgendorff, A., Reiss, I., Ehrhardt, H., Eickelberg, O. & Alvira, C. M. Chronic lung disease in the preterm infant: Lessons learned from animal models. *American Journal of Respiratory Cell and Molecular Biology* vol. 50 233–245 (2014).

51. Thébaud, B. *et al.* Bronchopulmonary dysplasia. *Nature Reviews Disease Primers* **5**, 78 (2019).

52. O'reilly, M. & Thébaud, B. Animal models of bronchopulmonary dysplasia. The term rat models. *Am J Physiol Lung Cell Mol Physiol* **307**, 948–958 (2014).

53. Berger, J. & Bhandari, V. Animal models of bronchopulmonary dysplasia. The term mouse models. *Am J Physiol Lung Cell Mol Physiol* **307**, 936–947 (2014).

54. Yoder, B. A., Coalson, J. J. & Yoder, B. A. Animal models of bronchopulmonary dysplasia. The preterm baboon models. *Am J Physiol Lung Cell Mol Physiol* **307**, 970–977 (2014).

55. Hilgendorff, A., Reiss, I., Ehrhardt, H., Eickelberg, O. & Alvira, C. M. Chronic lung disease in the preterm infant: Lessons learned from animal models. *American Journal of Respiratory Cell and Molecular Biology* vol. 50 233–245 (2014).

56. Salaets, T., Gie, A., Tack, B., Deprest, J. & Toelen, J. Modelling Bronchopulmonary Dysplasia in Animals: Arguments for the Preterm Rabbit Model. *Current Pharmaceutical Design* **23**, 5887–5901 (2017).

57. O'reilly, M. & Thébaud, B. Animal models of bronchopulmonary dysplasia. The term rat models. *Am J Physiol Lung Cell Mol Physiol* **307**, 948–958 (2014).

58. Albertine, K. H. & Albertine, K. H. Utility of large-animal models of BPD: chronically ventilated preterm lambs. *Am J Physiol Lung Cell Mol Physiol* **308**, 983–1001 (2015).

59. Joss-Moore, L. A. *et al.* Alveolar formation is dysregulated by restricted nutrition but not excess sedation in preterm lambs managed by noninvasive support. *Pediatric Research* **80**, 719–728 (2016).

60. George Gie, A. *et al.* Intermittent CPAP limits hyperoxia-induced lung damage in a rabbit model of bronchopulmonary dysplasia. *Am J Physiol Lung Cell Mol Physiol* **318**, 976–987 (2020).

61. Salaets, T., Gie, A., Tack, B., Deprest, J. & Toelen, J. Modelling Bronchopulmonary Dysplasia in Animals: Arguments for the Preterm Rabbit Model. *Current Pharmaceutical Design* **23**, 5887–5901 (2017).

62. Manzano, R. M. *et al.* A hyperoxic lung injury model in premature rabbits: The influence of different gestational ages and oxygen concentrations. *PLoS ONE* **9**, (2014).

63. Jiménez, J. *et al.* Progressive vascular functional and structural damage in a bronchopulmonary dysplasia model in preterm rabbits exposed to hyperoxia. *International Journal of Molecular Sciences* **17**, (2016).

64. Richter, J. *et al.* Functional assessment of hyperoxia-induced lung injury after preterm birth in the rabbit. *Am J Physiol Lung Cell Mol Physiol* **306**, 277–283 (2014).

65. Conway, R. F., Frum, T., Conchola, A. S. & Spence, J. R. Understanding Human Lung Development through In Vitro Model Systems. *BioEssays* **42**, (2020).

66. Otulakowski, G., Duan, W. & O'Brodovich, H. Global and gene-specific translational regulation in rat lung development. *American Journal of Respiratory Cell and Molecular Biology* **40**, 555–567 (2009).

67. Xu, Y. *et al.* Transcriptional programs controlling perinatal lung maturation. *PLoS ONE* **7**, (2012).

68. Ljungberg, M. C. *et al.* Spatial distribution of marker gene activity in the mouse lung during alveolarization. *Data in Brief* **22**, 365–372 (2019).

69. Beauchemin, K. J. *et al.* Temporal dynamics of the developing lung transcriptome in three common inbred strains of laboratory mice reveals multiple stages of postnatal alveolar development. *PeerJ* **2016**, (2016).

70. Moghieb, A. *et al.* Time-resolved proteome profiling of normal lung development. *Am J Physiol Lung Cell Mol Physiol* **315**, 11–24 (2018).

71. Cox, B. *et al.* Integrated proteomic and transcriptomic profiling of mouse lung development and Nmyc target genes. *Molecular Systems Biology* **3**, 109 (2007).

72. Jin, L. *et al.* Global long noncoding RNA and mRNA expression changes between prenatal and neonatal lung tissue in pigs. *Genes* **9**, (2018).

73. Yu, X. *et al.* Crosstalk of dynamic functional modules in lung development of rhesus macaques. *Molecular BioSystems* **12**, 1342–1349 (2016).

74. Kho, A. T. *et al.* Transcriptomic analysis of human lung development. *American Journal of Respiratory and Critical Care Medicine* **181**, 54–63 (2010).

75. Cooney, T. P. & Thurlbeck, W. M. The radial alveolar count method of Emery and Mithal: a reappraisal 2--intrauterine and early postnatal lung growth. *Thorax* **37**, 580–583 (1982).

76. ENAS A. A. ELHAFEZ, G. K. M. and M. M. H. Development of the respiratory acinus in the rabbit lung . *Recent Researches in Medicine and Medical Chemistry* (2012).

77. Xenia I. Roubliova, J. A. D. J. M. B. L. O. D. G. J. C. J. C. P. V. de V. D. T. and E. K. V. Morphologic changes and methodological issues in the rabbit experimental model for diaphragmatic hernia. *Histology and Histopathology Cellular and Molecular Biology* (2010).

78. Dobin, A. *et al.* STAR: ultrafast universal RNA-seq aligner. *Bioinformatics* **29**, 15–21 (2013).

79. Anders, S., Pyl, P. T. & Huber, W. HTSeq--a Python framework to work with high-throughput sequencing data. *Bioinformatics* **31**, 166–169 (2015).

80. Ritchie, M. E. *et al.* limma powers differential expression analyses for RNA-sequencing and microarray studies. *Nucleic Acids Research* **43**, e47–e47 (2015).

81. Langfelder, P. & Horvath, S. WGCNA: an R package for weighted correlation network analysis. *BMC Bioinformatics* **9**, 559 (2008).

82. Zhou, Y. *et al.* Metascape provides a biologist-oriented resource for the analysis of systems-level datasets. *Nature Communications* **10**, 1523 (2019).

83. Schittny, J. C. Development of the lung. *Cell and Tissue Research* vol. 367 427–444 (2017).

84. Mullassery, D. & Smith, N. P. Lung development. *Seminars in Pediatric Surgery* **24**, 152–155 (2015).

85. Hislop, A. Developmental biology of the pulmonary circulation. *Paediatric Respiratory Reviews* vol. 6 35–43 (2005).

86. Gao, Y. *et al.* Unique aspects of the developing lung circulation: Structural development and regulation of vasomotor tone. *Pulmonary Circulation* vol. 6 407–425 (2016).

87. Schittny, J. C. Development of the lung. *Cell and Tissue Research* vol. 367 427–444 (2017).

88. Wynne, K. *et al.* Antenatal corticosteroid administration for foetal lung maturation. *F1000Research* vol. 9 (2020).

89. Cai, Y. *et al.* Weighted Gene Co-expression Network Analysis of Key Biomarkers Associated With Bronchopulmonary Dysplasia. *Frontiers in Genetics* **11**, (2020).

90. Liu, W. *et al.* Weighted gene coexpression network reveals downregulation of genes in bronchopulmonary dysplasia. *Pediatric Pulmonology* **56**, 392–399 (2021).

91. Chen, M., Yan, J., Han, Q., Luo, J. & Zhang, Q. Identification of hub-methylated differentially expressed genes in patients with gestational diabetes mellitus by multi-omic WGCNA basing

epigenome-wide and transcriptome-wide profiling. *Journal of Cellular Biochemistry* **121**, 3173–3184 (2020).

92. Wan, H. *et al.* Compensatory roles of Foxal and Foxa2 during lung morphogenesis. *Journal of Biological Chemistry* **280**, 13809–13816 (2005).

93. Yeganeh, B. *et al.* Autophagy is required for lung development and morphogenesis. *Journal of Clinical Investigation* **129**, 2904–2919 (2019).

94. Bartram, U. & Speer, C. P. *The Role of Transforming Growth Factor in Lung Development and Disease**. www.chestjournal.org.

95. Saito, A., Horie, M. & Nagase, T. TGF-β signaling in lung health and disease. *International Journal of Molecular Sciences* vol. 19 (2018).

96. Rackley, C. R. & Stripp, B. R. Building and maintaining the epithelium of the lung. *Journal of Clinical Investigation* vol. 122 2724–2730 (2012).

97. Yao, J. *et al.* Vascular endothelium plays a key role in directing pulmonary epithelial cell differentiation. *Journal of Cell Biology* **216**, 3369–3385 (2017).

98. le Cras, T. D. *et al.* Treatment of newborn rats with a VEGF receptor inhibitor causes pulmonary hypertension and abnormal lung structure. *Am J Physiol Lung Cell Mol Physiol* **283**, 10 (2002).

99. Schultz, C. J., Torres, E., Londos, C. & Torday, J. S. Role of adipocyte differentiation-related protein in surfactant phospholipid synthesis by type II cells. *Am J Physiol Lung Cell Mol Physiol* **283**, 288–296 (2002).

100. Han, S. H. & Mallampalli, R. K. The role of surfactant in lung disease and host defense against pulmonary infections. *Annals of the American Thoracic Society* vol. 12 765–774 (2015).

101. Hooper, S. B. *et al.* Cardiovascular transition at birth: A physiological sequence. *Pediatric Research* vol. 77 608–614 (2015).

102. Schachtner, S. K., Wang, Y. & Scott Baldwin, H. *Qualitative and Quantitative Analysis of Embryonic Pulmonary Vessel Formation*. *Am. J. Respir. Cell Mol. Biol* vol. 22 www.atsjournals.org (2000).

103. Strueby, L. & Thébaud, B. Advances in bronchopulmonary dysplasia. *Expert Review of Respiratory Medicine* vol. 8 327–338 (2014).

104. Schittny, J. C., Mund, S. I. & Stampanoni, M. Evidence and structural mechanism for late lung alveolarization. *Am J Physiol Lung Cell Mol Physiol* **294**, 246–254 (2008).

105. Narayanan, M. *et al.* Alveolarization continues during childhood and adolescence: New evidence from helium-3 magnetic resonance. *American Journal of Respiratory and Critical Care Medicine* **185**, 186–191 (2012).

106. Baker, C. D. & Alvira, C. M. Disrupted lung development and bronchopulmonary dysplasia: Opportunities for lung repair and regeneration. *Current Opinion in Pediatrics* vol. 26 306–314 (2014).

107. Granese, R. *et al.* Preterm birth: Seven-year retrospective study in a single centre population. *Italian Journal of Pediatrics* **45**, (2019).

108. Glass, H. C. *et al.* Outcomes for extremely premature infants. *Anesthesia and Analgesia* **120**, 1337–1351 (2015).

109. Beck, S. *et al.* The worldwide incidence of preterm birth: A systematic review of maternal mortality and morbidity. *Bulletin of the World Health Organization* **88**, 31–38 (2010).

110. Salaets, T. *et al.* Preterm birth impairs postnatal lung development in the neonatal rabbit model. *Respiratory Research* **21**, (2020).

111. Lee, J. W. & Davis, J. M. Future applications of antioxidants in premature infants. *Current Opinion in Pediatrics* **23**, 161–166 (2011).

112. Gopinathan, V., Miller, N. J., Milner, A. D. & Rice-Evans, C. A. Bilirubin and ascorbate antioxidant activity in neonatal plasma. *FEBS Letters* **349**, 197–200 (1994).

113. Zhuang, T., Zhang, M., Zhang, H., Dennery, P. A. & Lin, Q. S. Disrupted postnatal lung development in heme oxygenase-1 deficient mice. *Respiratory Research* **11**, (2010).

114. R J Martin, J. M. D. F. P. M. M. C. G. W. Physiologic basis for intermittent hypoxic episodes in preterm infants. *Adv Exp Med Biol* (2012).

115. Jobe, A. H. Mechanisms of Lung Injury and Bronchopulmonary Dysplasia. *American Journal of Perinatology* vol. 33 1076–1078 (2016).

116. Kalikkot Thekkeveedu, R., Guaman, M. C. & Shivanna, B. Bronchopulmonary dysplasia: A review of pathogenesis and pathophysiology. *Respiratory Medicine* vol. 132 170–177 (2017).

117. Kajekar, R. Environmental factors and developmental outcomes in the lung. *Pharmacology and Therapeutics* vol. 114 129–145 (2007).